Financial flights, stock market linkages and jump excitation[☆]

Mardi Dungey[a], Deniz Erdemlioglu[b,*], Marius Matei[a], Xiye Yang[c]

[a] *Tasmanian School of Business and Economics, University of Tasmania, Australia*
[b] *IESEG School of Management and CNRS, France*
[c] *Department of Economics, Rutgers University, U.S.*

This Version: June 24, 2016

Abstract

We propose a new nonparametric test to identify the mutually exciting jumps in high frequency data. We derive the asymptotic properties of the test statistics and show that the tests behave reasonably well in finite sample cases. Using our mutual excitation tests, we characterize global stock market linkages and study the dynamics of financial flights. The results suggest that flight-to-safety episodes (from stocks to gold) occur more frequently than do flight-to-quality cycles (from stocks to bonds). The excitation channel further appears to be asymmetric at high frequency: emerging market jumps excite U.S. equities, and the evidence supporting the reverse transmission is quite weak. The data exhibit a strong excitation effect from volatility jumps to price jumps.

Keywords: Flight-to-safety, Flight-to-quality, Mutual-excitation in jumps, Financial contagion, Stock-bond comovement, Asset market linkages, Financial crises, High-frequency data, Volatility feedback effect

JEL: G01, G12, G15, C12, C14, C58

[☆]We thank Massimiliano Caporin, Pasquale Della Corte, Ozgur Demirtas, Dobrislav Dobrev, Louis Eeckhoudt, Robert Engle, Neil R. Ericsson, Andrew Harvey, David F. Hendry, Sébastien Laurent, Simone Manganelli, Christopher J. Neely, Marc Paolella, Andrew Patton, Olivier Scaillet, Paul Schneider, Victor Todorov, Giovanni Urga, Lars Winkelmann, Kamil Yilmaz and participants at the 9th Annual SoFiE Conference, IAAE 2016 Annual Conference, Federal Reserve Bank of St. Louis Research Seminar and 16th Oxmetrics Financial Econometrics Conference for valuable comments and helpful suggestions. Dungey and Matei acknowledge funding from Australian Research Council grant (DP130100168).

[*]Corresponding author. IÉSEG School of Management, 3 Rue de la Digue, Lille, France. Tel: +33 (0)320 545 892. Fax: +33 (0)320 574 855.

Email addresses: mardi.dungey@utas.edu.au (Mardi Dungey), d.erdemlioglu@ieseg.fr (Deniz Erdemlioglu), marius.matei@utas.edu.au (Marius Matei), xiyeyang@econ.rutgers.edu (Xiye Yang)

1. Introduction

> "*U.S. and European stocks dived after a sharp selloff in Chinese shares accelerated, wiping out gains for the year. Oil prices continued to drop, while Treasurys gained as investors sought the relative safety of government bonds.*"
>
> (*Wall Street Journal*, August 24, 2015, 3:55 pm−EST)

> "*This is a flight to quality and the actual level that the Treasury yield achieves in this environment is not meaningful. This is a time when you dig a deep hole, close your eyes and put your fingers in your ears.*"
>
> (David Keeble, Crédit Agricole, *Wall Street Journal*, August 24, 2015, 4:24 pm−EST)

The global financial system is vulnerable to unforeseen shocks and unexpected events. Sudden shocks may, for instance, amplify uncertainty, which, in turn, exacerbates fear and increases risk perception in the marketplace. The downside effects of financial stress could be even worse, especially when the shocks in one region (or market) spread to others through contagion and market linkages.[1]

Over the last two decades, financial markets have experienced various adverse shocks and sudden crashes. East Asian countries, for instance, were hit by severe financial turmoil during 1997-98, triggering currency crises and plunges in stock markets in that region. Shortly after the Asian crisis, the Russian government defaulted on its debt on August 17, 1998, and this event accelerated the collapse of the hedge fund Long-Term Capital Management (LTCM). Argentina suffered from a great depression and sharp recession in the beginning of 2000s. More recently, in the United States, the House voted against the bailout of Lehman Brothers on September 29, 2008. As Figure 1 displays, the market reaction to this event was rather swift at the intraday level: the S&P 500 index declined sharply around 18:00 GMT, within minutes after the news shock, and the VIX index—a common proxy for market volatility—elevated substantially.

[Insert Figure 1 about here]

How do such historical tail events propagate from one location (or market) to another? What is the degree of transmission, when does it occur and why do we observe contagion? These questions are important for the measurement of market risk (embedded in risk spillovers), credit risk (associated with default spillovers) and systemic/system-wide risk (linked to tail comovements). For portfolio managers, understanding the linkages of shocks (e.g., between bonds and stocks) is of

[1] Researchers define the term *financial contagion* in different ways. Forbes and Rigobon (2002) argue that financial contagion is an increase in cross-market comovement after a sudden shock to one market (or country). If correlation does not increase significantly, it creates only interdependence. Dungey and Martin (2007) separate contagion from spillover. The difference between two types of linkages is related to the timing of transmission. While contagion refers to a shock transmission occurring contemporaneously between two markets, spillovers arrive with time lags. Dungey and Martin (2007) further show that spillover effects are larger than contagion effects.

interest to evaluate asset allocation and diversification strategies. The risk exposure of portfolios to sudden global shocks, for instance, depends on the dynamics of linkages. From an option pricing perspective, derivative analysts consider shock spillovers when valuing derivative securities whose payoffs typically rely on multiple asset prices.

The literature offers two main directions to study financial contagion. One strand investigates the sources of shocks that can be linked to information arrivals (Harvey and Huang, 1991, Ederington and Lee, 1993, King and Wadhwani, 1990, Calvo and Mendoza, 2000), liquidity or trading activity (Diamond, 1983, Caballero and Krishnamurthy, 2008, Jiang et al., 2011, Fleming et al., 1998). While Dungey et al. (2010), for instance, consider structural shocks as main market crash drivers, Allen and Gale (2000) exploit the characteristics of real shocks; the innovations to preferences and consumer behavior in one particular country or asset class.

Another body of research focuses on the measurement of asset market linkages.[2] These studies propose using statistical and econometric methods to analyze financial contagion. For example, Forbes and Rigobon (2002) investigate the correlation between global stock markets and find relatively weak evidence of contagion.[3] Pelletier (2006) extends this work and considers different regime structures in examining cross correlations. Compared to the multivariate analysis of Evans (2002), Pelletier (2006) documents smoother correlations across major foreign exchange rates. Chan et al. (2011) focus on multiple asset classes and show the presence of cross linkages. While Guidolin and Timmermann (2006, 2007) characterize the nonlinear dynamics of the stock-bond relation, King and Wadhwani (1990) and, more recently, Diebold and Yilmaz (2014) examine the transmission of volatility within stock markets.[4] These studies suggest that financial volatility exhibits strong connectedness that varies over time with market conditions.

Despite the substantial progress, relatively little is known about the spillover of *abnormal (jump-type)* shocks for several potential reasons. The first reason is broadly linked to a model selection problem. In practice, the process generating shocks is latent; hence, jumps are not directly observable. This (model uncertainty) problem arises, particularly when researchers seek to exploit the patterns in high-frequency data. As Aït-Sahalia and Jacod (2012) point out, tail-type jump events tend to occur more frequently at short time scales compared to long investment horizons. Therefore,

[2]The literature on this direction is rather vast. For currency market linkages, see, e.g., Diebold and Nerlove (1989), Mahieu and Schotman (1994), Kaminsky and Reinhart (2000); for stock market linkages, see, e.g., Bae et al. (2003), Forbes and Rigobon (2002), King and Wadhwani (1990), King et al. (1994), Lin et al. (1994), Karolyi (1995), Bekaert et al. (2005), Hamao and Ng (1990), Karolyi and Stulz (1996); and for bond market linkages, see, e.g., Favero and Giavazzi (2002) and Dungey et al. (2000).

[3]In the literature on asset market linkages, researchers classify contagion in several ways: (i) contagion across countries for a single asset class (e.g., Bae et al., 2003, Karolyi and Stulz, 1996, Karolyi, 1995, Hamao and Ng, 1990), (ii) contagion across different asset classes within a particular region (e.g., Chan et al., 2011), and (iii) contagion across different countries and asset classes (e.g., Hartmann et al., 2004, Forbes and Chinn, 2004, Dungey and Martin, 2007). See also Baur (2012), who studies the effect of financial contagion on the real economy by considering both developed and emerging stock markets.

[4]See also Longin and Solnik (1995), Hamao and Ng (1990) and Flood and Rose (2005). Longin and Solnik (1995) is an example of earlier works suggesting time-varying cross-market correlations. Hamao and Ng (1990) and, more recently, Flood and Rose (2005) analyze the covariance between international stock markets and within the U.S., respectively.

a model that fails to characterize jump linkages at a relatively high frequency might underestimate the true dependence in shocks. The second challenge is related to the empirical characteristics of volatility. In financial data, one might notice that the periods of high volatility mingle with the periods of co-jumps. This is not surprising because sudden crashes might trigger fear and turbulence, which, in turn, increase market-wise volatility. Such patterns, however, create complications for the estimation of market risk embedded in jump spillovers and volatility transmission. It is thus crucial to separate joint jump shocks from volatility linkages. Perhaps more importantly, those jump-type shocks are likely to propagate over time (e.g., during the crisis), and tail events may spread with delay. In the presence of such regularities, understanding the origin (or direction) of jump spillovers may be difficult and ambiguous. Although correlation/covariance-based measures are certainly of interest in this context, jump-type shock transmission remains elusive.

In this paper, we address these issues and develop a new approach to measure the transmission of jumps in financial markets. Relying on nonparametric (model-free) testing procedures, this approach allows us to characterize the dynamic properties of shock transmission in greater depth than is possible with correlation/covariance analysis or traditional co-jump techniques. In our continuous-time setup, jump-type shocks in one financial asset (or region) have the potential to cluster over time and to increase the intensity of jumps in other assets (*mutual excitation*). We derive the asymptotic behavior of these mutual excitation tests and assess their finite sample performance via simulations. Applying the tests to high-frequency data, we study episodes of *financial flights* (i.e., risk-on-risk-off trades), measure *directional* stock market linkages and examine the link between jumps in volatility and jumps in asset prices.

Our paper makes three contributions to the extant literature. First, we propose a new nonparametric test for identifying common jump arrivals in high-frequency data. Our econometric procedure is particularly related to the multivariate tests of Bollerslev et al. (2008), Jacod and Todorov (2009), Mancini and Gobbi (2012) and Bibinger and Winkelmann (2015). Among these studies, Bollerslev et al. (2008) identify cojumps by utilizing cross-covariance of asset returns. Jacod and Todorov (2009) extend the test of Bollerslev et al. (2008) to a generalized framework based on two possible hypotheses (common jumps or disjoint jumps). The study by Mancini and Gobbi (2012) is the first to develop the formal truncation method to pin down cojumps. Building on Jacod and Todorov (2009) and Mancini and Gobbi (2012), the cojump analysis of Bibinger and Winkelmann (2015) accounts for non-synchronous trading and market microstructure noise in the data. Perhaps surprisingly, these studies consider jumps as *Lévy-type* (i.e., either Poisson or pure Lévy), and hence, cojumps occur randomly (in theory) with no memory.[5] Moreover, the statistical problem is typically assumed to be symmetric in the literature, that is, jumps arrive simultaneously and the origins of shocks may be negligible. We relax these assumptions and minimize these

[5]Empirically, several studies link cojumps to news announcements. For example, Lahaye et al. (2011) consider various asset classes and find evidence that macro news creates cojumps. Dungey and Hvozdyk (2012) focus on the U.S. Treasury bond market and study cojumps between spot prices and futures. Bibinger et al. (2015) use ECB monetary policy surprises to explain cojump patterns in interest rates.

restrictions on jump dynamics. In a rather tractable specification, we allow the jumps in one asset to increase the jump intensity of the other asset, not necessarily contemporaneously but with lags. Cojumps are *directional* events in our identification. For instance, while the jumps in asset A excite the shock occurrences in asset B, the reverse directional effect may not hold in practice (i.e., from B to A). As we shall discuss later, we propose *four* different tests for the *four* possible null hypotheses (absence of jump excitation from A to B, or B to A; presence of jump excitation from A to B, or B to A). We develop the concept, derive the asymptotic properties of the test statistics and show that the tests behave reasonably well in finite sample cases.

[Insert Figure 2 about here]

Second, we study the dynamics of financial flights associated with *mutually exciting* jump-type tail events. Researchers often define *flights* as periods of risk-off trades, when market participants flee relatively risky investments (such as stocks) and invest in safe assets (i.e., flight to safety (FTS)) or assets of high quality (i.e., flight to quality (FTQ)). As widely reported in the media, these episodes typically occur when market conditions abruptly deteriorate due to certain political or news events.[6] Figure 2 illustrates an example of an intraday financial flight that occurred on August 5-6, 2014, when the tension in the Middle Eastern and Ukraine-Russia conflicts increased significantly. In the figure, the Bloomberg trading screen exhibits a sharp sudden decline in the index—around 19:30 GMT—as gold prices surged rapidly. Studying financial flights is of interest not only in terms of understanding the behavior of investors but also in terms of measuring risk transmission (and premia) within the global financial system. Recent academic research has focused on the identification and determinants of these events. For instance, Caballero and Krishnamurthy (2008) develop a theoretical model and show that unusual and unexpected events lead to FTQ trades. Baele et al. (2014) confirm this view empirically by identifying international FTS. In this direction, Goyenko and Sarkissian (2015) consider U.S. macroeconomic shocks to be drivers of FTQ. Engle et al. (2012) focus on the market microstructure and examine the dynamics of the U.S. Treasury market around FTS periods.[7] Unlike Baele et al. (2014) and Goyenko and Sarkissian (2015), we characterize financial flights at the intraday level. High-frequency data allow us to more precisely measure the arrivals (and magnitudes) of large adverse shocks in assets. While Longstaff (2004) and Engle et al. (2012) focus on the U.S. Treasury market, we examine not only bonds but also stocks and commodities. Compared to these studies, the identification approach in this

[6] For instance, Bloomberg reported the following headline on July 10, 2014 at 4:03 pm−EST. "*Stocks from U.S. to Europe slid as increasing concern over signs of financial stress in Portugal sent investors seeking safety in Treasuries, the yen and gold.*"

[7] In this paper, we restrict our attention to the dynamics of FTS and FTQ. It is worth noting that financial flights could also come in other forms, such as flight to liquidity (FTL) trades. In this alternative direction, Vayanos (2004) develops an equilibrium model and shows that risk aversion increases during periods of turmoil, and investors experience a sudden and strong preference for holding bonds. Liquidity premium is time-varying and increases with volatility. Extending this approach, Brunnermeier and Pedersen (2009) theoretically link market liquidity to FTQ. Beber et al. (2009) analyze European bond market and provide evidence that investors demand credit liquidity—rather than quality—in times of crisis: FTL dominates FTQ. From an empirical perspective, Longstaff (2004) studies the risk premium implications of FTL in the U.S. Treasury bond market.

paper is non-parametric and flexible enough to capture the different strengths of shocks and time variation in FTS/FTQ regimes. Our empirical analysis reveals that FTS periods (from stocks to gold) occur more frequently than FTQ cycles (from stocks to bonds). Interestingly, however, as adverse shocks become severe, the activity of financial flights decreases substantially. In addition, we explore *seeking returns strategies* (SRS) used by investors when risk appetite increases in the marketplace. We find evidence of such SRS patterns in the data. The results suggest that SRS episodes exhibit asymmetry, likely reflecting the fact that as market conditions improve, traders prefer to sell gold, rather than bonds, to invest in stocks.

The third contribution of the paper is the analysis of the stock-bond relationship and asset market linkages. In the stock-bond literature, our paper is particularly related to the studies by Panchenko and Wu (2009), Baele et al. (2010) and Bansal et al. (2014).[8] Panchenko and Wu (2009) link stock-bond comovements to emerging market integration.[9] Estimating a dynamic factor model with quarterly data, Baele et al. (2010) show that the drivers of stock-bond comovements are mostly liquidity and uncertainty factors, and the role of fundamental/macro information is quite weak. Bansal et al. (2014) conclude that negative stock-bond correlations are due to stronger link between risk and returns. Our empirical analysis is based on high-frequency data, and we examine the stock-bond relationship associated with jump-type tail events rather than correlations. Like Bae et al. (2003), we consider the possibility that severe shocks may propagate differently from small shocks. However, while Bae et al. (2003) utilize extreme value theory based on low-frequency return distribution, we adopt a nonparametric approach relying on continuous time. Our sample is larger and more recent than that used by Bae et al. (2003). Investigating global stock market integration, we provide evidence that the linkages between developed and emerging stock markets are considerably *asymmetric*. In particular, we find that jump-type events hitting Latin American stocks tend to excite U.S. stocks and that evidence supporting reverse transmission is rather weak. This result confirms the view of Bae et al. (2003) but contradicts the conclusions by Aït-Sahalia et al. (2014). The trading frequency—short or long—thus becomes crucial in identifying the direction of cross-border spillover effects.

This paper is even more closely related to the studies that empirically analyze linkages during crisis periods and financial turmoil (e.g., Hartmann et al., 2004, Dungey and Martin, 2007 and Glick and Hutchison, 2013). Glick and Hutchison (2013) document strong stock market linkages between China and Asia around the 2008-2009 crisis. Hartmann et al. (2004) estimate the tail dependence between stock and bond markets of G-5 countries. The analysis by Hartmann et al. (2004) is based on weekly data over the 1987-1999 period (i.e., around 663 weekly returns). Our approach, however, focuses relatively more on recent market conditions (2007-2013) and detects

[8]For other specifications to test for market linkages and stock-bond comovements, see, e.g., Andersen et al. (2007), Forbes and Rigobon (2002), Hartmann et al. (2004), Chordia et al. (2005), Connolly et al. (2005), Kim et al. (2006) and Karolyi and Stulz (1996).

[9]For other studies analyzing emerging market integration, see, e.g., Bekaert and Harvey (1995, 1997, 2000) and De Jong and De Roon (2005).

linkages from intraday data (i.e., around 141,000 5-minute returns). To identify tail spillovers, Hartmann et al. (2004) calculate the *expected* number of crashes given other market crashes. The testing procedure by Hartmann et al. (2004) is thus *ex ante*, whereas we utilize *ex post* realized measures in continuous time, such as integrated volatility and threshold power variation. We find evidence of *cross-excitation* in jump tails between (i) U.S. stocks and U.S. bonds, (ii) U.S. stocks and emerging market stocks, and (iii) market volatility and asset prices. Our results suggest that stock market linkages are relatively strong in times of turbulent periods, such as the liquidity case of BNP Paribas, the bankruptcy of Lehman Brothers, the rescue of AIG, the implementation of the Trouble Assets Relief Program, and the intensification of the European debt crisis (2011-2012).

The theoretical contribution of this paper builds directly on Boswijk et al. (2014). Our bivariate (mutual excitation) analysis extends the univariate (self-excitation) approach of Boswijk et al. (2014). Further, we show that the asymptotic behavior of the test statistics remain fairly similar to that of self-excitation tests. Boswijk et al. (2014) measure self-excitation in jumps of a single asset. In contrast, we are interested in testing for mutual excitation in jumps *between* (at least) two assets. Therefore, our approach identifies the jump propagation in space, whereas Boswijk et al. (2014) examine jump propagation in time.

Our paper extends Aït-Sahalia et al. (2014) and Aït-Sahalia et al. (2014b) in several respects. In contrast to the parametric model specifications of these studies, our approach is nonparametric and relies on test statistics that are model-free. This feature allows us to be flexible in characterizing the (bivariate) log-price process: the coefficients of the diffusion terms, volatility components, jump sizes, and jump intensity process can be in any (semimartingale) form. We derive the asymptotic behavior (level and power) of the test statistics and consider different null hypotheses to identify the periods of mutual excitation in the data.

Aït-Sahalia et al. (2014) and Aït-Sahalia et al. (2014b) consider a finite jump activity for the underlying Hawkes-type return variation. We relax this assumption in our methodological setup: jumps can exhibit infinite activity with mutual excitation. We can thus generalize the dynamics of jump-type financial shocks in a rather comprehensive way. Shocks can be large (and rare) or small (and frequent). Furthermore, we vary the jump size (i.e., the excitation threshold) and, hence, capture different levels of jump propagation in the form of weak, mild or severe transmissions.

On the methodological side, our model setup is based entirely on continuous-time. Unlike Aït-Sahalia et al. (2014) and Aït-Sahalia et al. (2014b), we rely on intraday data—rather than daily data—to test for cross-excitation across assets. The use of high-frequency data gives us more accurate information about the realized return characteristics, latent (spot) market volatility and jump dynamics. On the empirical front, Aït-Sahalia et al. (2014) and Aït-Sahalia et al. (2014b) study mutual excitation in international stock markets and European sovereign CDS, respectively. Instead, our focus is the excitation channel between U.S. and emerging stock indices, commodities and long-term debt securities. We identify FTS and FTQ fund flows in financial markets using our mutual excitation tests. Implementing this approach, we further provide evidence of *leverage* and *volatility feedback* effects associated with jumps and excitations.

The remainder of this paper is organized as follows. Section 2 introduces the formal setup, the base methodology and testing procedures. In Section 3, we present the Monte Carlo simulations to assess the finite sample performance of the tests. Section 4 describes the data and reports our empirical results. We check the robustness of our results in Section 5. Section 6 concludes.

2. Methodology

2.1. Excitation dynamics of jump-type shocks

Our objective is to identify the transmission of large shocks from one asset (or region) to another. Before introducing our formal setup, we first illustrate the excitation dynamics as in Aït-Sahalia et al. (2014) and Aït-Sahalia et al. (2014b). Consider two assets ($d = 1, 2$) and let the log-price of each asset follow a semimartingale Itô:

$$dX_{d,t} = \mu_{d,t}dt + \sigma_{d,t}dW_{d,t} + \xi_{d,t}dN_{d,t}, \qquad d = 1, 2, \tag{1}$$

with a *Hawkes-type* jump intensity process

$$d\lambda_{d,t} = \tilde{\alpha}_d(\lambda_{d,\infty} - \lambda_{d,t})dt + \sum_{l=1}^{2} \tilde{\beta}_{d,l}dN_{l,t}, \qquad d, l = 1, 2, \tag{2}$$

where $\mu_{d,t}$ is the drift term, $\sigma_{d,t}$ is the stochastic volatility component, and $W_{d,t}$ denotes a standard Brownian motion. In (1), $\xi_{d,t}$ denotes the jump size at time t and $N_{d,t}$ is a Hawkes process for each asset $d = 1, 2$. The intensity of jumps follows the dynamics in (2) with conditions $\tilde{\alpha}_d > \tilde{\beta}_{d,l} > 0$ and $\lambda_{d,\infty} > 0$ for $d, l = 1, 2$.[10] For ease of exposition, we can rewrite (2) as

$$\lambda_{1,t} = \lambda_{1,\infty} + \int_{-\infty}^{t} \tilde{\beta}_{1,1}e^{-\tilde{\alpha}_1(t-s)}dN_{1,s} + \int_{-\infty}^{t} \tilde{\beta}_{1,2}e^{-\tilde{\alpha}_1(t-s)}dN_{2,s}, \tag{3}$$

$$\lambda_{2,t} = \lambda_{2,\infty} + \int_{-\infty}^{t} \tilde{\beta}_{2,1}e^{-\tilde{\alpha}_2(t-s)}dN_{1,s} + \int_{-\infty}^{t} \tilde{\beta}_{2,2}e^{-\tilde{\alpha}_2(t-s)}dN_{2,s}, \tag{4}$$

where $\lambda_{1,t}$ and $\lambda_{2,t}$ are the shock intensity processes of assets 1 and 2, respectively. The intuition behind the setup in (3)−(4) is the following. Consider the jump dynamics of asset 1 (i.e., Equation (3)). Whenever a sudden shock ($dN_{2,s} = 1$) occurs in asset 2, $\lambda_{1,t}$ jumps with magnitude $\tilde{\beta}_{1,2}$. The jump intensity $\lambda_{1,t}$ then mean-reverts back towards $\lambda_{1,\infty}$ at speed $\tilde{\alpha}_1$. This specification delivers two types of feedback mechanism. First, the jump intensity of each asset changes over time and responds to past jumps (via $\tilde{\beta}_{1,1}$ and $\tilde{\beta}_{2,2}$). This is the *self-excitation* of jumps. Second, jump events in one asset propagate across markets and increase the chance of future shocks in other assets (via $\tilde{\beta}_{1,2}$ and $\tilde{\beta}_{2,1}$). The latter effect is the *mutual excitation* that we wish to capture. The next section now introduces our modeling framework.

[10] These conditions ensure that intensities of shocks follow stationary Markov processes.

2.2. The model setup

Throughout, we fix a probability space $(\Omega, \mathcal{F}_t, \mathbb{P})$ where Ω is the set of events in financial markets, $\mathcal{F}_t : t \in [0,T]$ is (right-continuous) information filtration for investors, and $\mathbb{P}$ is a data-generating measure. We follow Boswijk et al. (2014) and consider the *Grigelionis decomposition* of $X_{d,t}$ in (1). That is,

$$X_{d,t} = X_{d,0} + \int_0^t b_{d,s} ds + \int_0^t \sigma_{d,s} dW_{d,s} + x_d * (\mu_{d,t} - \nu_{d,t}) + (x_d - h(x_d)) * \mu_{d,t}, \tag{5}$$

where $b_d = (b_{d,t})$ and $\sigma_d = (\sigma_{d,t})$ are locally bounded, μ_d is the jump measure of X_d and ν_d is its jump compensator that adopts the following decomposition

$$\nu_d(dt, dx) = dt \otimes F_{d,t}(dx).$$

We further assume that the predictable random measure $F_{d,t}$ can be factored into two parts:

$$F_{d,t}(dx) = f_{d,t}(x)\, \lambda_{d,t-}\, dx. \tag{6}$$

Here, the predictable function $f_{d,t}(x)$ controls the jump size distribution and $\lambda_{d,-} = (\lambda_{d,t-})$ [11] is the stochastic jump intensity or stochastic scale, where

$$\lambda_{d,t} = \lambda_{d,0} + \int_0^t b'_{d,s} ds + \int_0^t \sigma'_{d,s} dW_{d,s} + \int_0^t \sigma''_{d,s} dB_{d,s} + \delta_{d,1} * \mu_{1,t} + \delta_{d,2} * \mu_{2,t} + \delta'' * \mu^{\perp}_{d,t}, \tag{7}$$

where B is a standard Brownian motion independent of W, $\mu^{\perp}_d$ is orthogonal to μ_1 and μ_2, and $\delta_{d,1}$, $\delta_{d,2}$, δ''_d are predictable. Boswijk et al. (2014) identify self-excitation through the common jumps between a log price process X and its own jump intensity λ.[12] We extend their framework to test for mutual excitation in jumps across assets. Consider a function of, for example, X_1 and λ_2 as follows.

$$U(H)_t = \sum_{0 \le s \le t} H(X_{1,s-}, X_{1,s+}, \lambda_{2,s-}, \lambda_{2,s+}). \tag{8}$$

The idea is then to choose a function H for $\mathbb{R} \times \mathbb{R} \times \mathbb{R}^*_+ \times \mathbb{R}^*_+$ such that $U(H)_T$ behaves distinctly when X_1 and λ_2 (the jump intensity of X_2) do or do not co-jump within the interval $[0,T]$. For instance, one may choose a function H such that

$$H(x_1, x_2, y_1, y_2) = 0 \iff x_1 = x_2 \text{ or } y_1 = y_2, \tag{9}$$

[11] For each $t > 0$, $\lambda_{d,t-} := \lim_{s \uparrow t} \lambda_{d,t}$. Similarly, $\lambda_{d,t+} := \lim_{s \downarrow t} \lambda_{d,t}$.

[12] See Aït-Sahalia and Hurd (2016) for an alternative model of optimal portfolio selection when jumps are mutually exciting. While Li et al. (2016, 2014) use jump regressions to identify jump size dependence (based on constant intensity), we focus on the interaction between jumps and time-varying jump intensity process. In this direction, Corradi et al. (2014) propose a self-excitement test for constant jump intensity in asset returns.

or

$$H(x_1, x_2, y_1, y_2) \neq 0 \Longleftrightarrow x_1 \neq x_2 \text{ and } y_1 < y_2, \tag{10}$$

or even more specifically, one can consider

$$H(x_1, x_2, y_1, y_2) \begin{cases} > 0 & \text{if } x_1 \neq x_2 \text{ and } y_1 < y_2, \\ = 0 & \text{if } x_1 = x_2 \text{ or } y_1 = y_2, \\ < 0 & \text{if } x_1 \neq x_2 \text{ and } y_1 > y_2. \end{cases} \tag{11}$$

Remark 1. If at a time point t, we have $|\Delta X_{1,t}| = 0$, then no matter which above condition H satisfies, the value of H at this time point is zero. If $|\Delta X_{1,t}| \neq 0$, then H will take different values according to whether $\Delta\lambda_{2t}$ is equal to, greater than, or smaller than zero. We summarize the sign of H for each case in Table 1.[13]

[Insert Table 3 about here]

Remark 2. A complication may arise when $|\Delta X_{1,t}|\,\Delta\lambda_{2,t} > 0$ and $|\Delta X_{2,t}| \neq 0$. That is, the positive jump in $\lambda_{2,t}$ may come from the jump in $X_{1,t}$, $X_{2,t}$ or both. In this case, it is not possible to disentangle the effect of $X_{1,t}$ and that of $X_{2,t}$. However, many common jumps indicate that other driving forces might trigger these common jumps.[14]

One challenge here is that the jump intensity process is not observable. To determine the value of H at each jump time of X_1, we need to estimate the spot values of λ_2 before and after this jump time. To achieve this goal and define *mutual excitation* in jump-type shocks, we make the following assumption for $F_{d,t}$ (in (6)).

Assumption 1. *Suppose the drift and volatility processes $b_{d,t}$ and $\sigma_{d,t}$ ($d = 1, 2$) are locally bounded. Assume that there are three (nonrandom) numbers $\beta_d \in (0, 2)$, $\beta'_d \in [0, \beta_d)$ and $\gamma > 0$, and a locally bounded process $L_t \geq 1$, such that, for all (ω, t),*

$$F_{d,t} = F'_{d,t} + F''_{d,t}, \tag{12}$$

where

(a) $F'_{d,t}(dx) = f_{d,t}(x)\lambda_{d,t-}dx$ with $\lambda = (\lambda_{d,t})$ given by (7), $\lambda_{d,t} \leq L_t$ and

$$f_{d,t}(x) = \frac{1 + |x|^{\gamma} h_d(t, x)}{|x|^{1+\beta}}, \tag{13}$$

[13] In practice, we believe that it is quite unlikely to have $\Delta\lambda_{2t} < 0$ when $|\Delta X_{1,t}| \neq 0$. In other words, the likelihood that a jump in X_1 will decrease the intensity of X_2 is very small because price jumps rarely stabilize financial market conditions.

[14] It is worth noting that we are not making causal inferences here. We are particularly interested in tracing whether or not the jumps in X_1 will be accompanied by a positive jump in the intensity of X_2.

for some predictable function $h_d(t,x)$*, satisfying*

$$1 + |x|^{\gamma} h_d(t,x) \geq 0, \quad |h_d(t,x)| \leq L_t. \tag{14}$$

(b) $F''_{d,t}$ *is a measure that is singular with respect to* F'_t *and satisfies*

$$\int_{\mathbb{R}} (|x|^{\beta'} \wedge 1) F''_{d,t}(dx) \leq L_t. \tag{15}$$

Given these dynamics, we assume that the log-price process $X_{d,t}$ in (1) is observed at discrete points in time. For each asset ($d = 1, 2$), the continuously compounded i-th intraday return of a trading day t is given by $r_{t,i} \equiv X_{(t+i\Delta_n)} - X_{(t+(i-1)\Delta_n)}$, with $i = 1, ..., M$ and trading days $t = 1, ..., T$. Let $M \equiv \lfloor 1/\Delta_n \rfloor$ denote the number of intraday observations in one day. $\Delta_n = 1/M$ is then the time between consecutive observations, the inverse of the observation frequency. To characterize mutual excitation, we introduce a testing procedure that relies on certain functional forms and jump intensity estimators. Extending the methodological framework of Boswijk et al. (2014), we begin by defining these measures.

Definition 1. *For each asset* $d = 1, 2$*, let* $U(H)_t$ *denote the functional of* X_t *in (1). The estimator of* $U(H)_t$ *is then given by*

$$U(H, k_n)_t^{12} = \sum_{i=k_n+1}^{[t/\Delta_n]-k_n} H(X_{1,i-1}, X_{1,i}, \widehat{\lambda}(k_n)_{2,i-}, \widehat{\lambda}(k_n)_{2,i}) 1_{\{|\Delta_i^n X_1| > \alpha \Delta_n^{\varpi}\}}, \tag{16}$$

where k_n *is an integer and* $\alpha\Delta_n^{\varpi}$ *is the truncation threshold indexed by* α *(*> 0*) for a constant (*$0 < \varpi < 1/2$*).*

In the functional form (16), $\widehat{\lambda}(k_n)$ is the estimator of the (spot) jump intensity λ_t given by

$$\widehat{\lambda}(k_n)_{2,i} = \frac{\Delta_n^{\varpi\beta_2}}{k_n \Delta_n} \sum_{j=i+1}^{i+k_n} g\left(\frac{|\Delta_j^n X_2|}{\alpha \Delta_n^{\varpi}}\right) \frac{\alpha^{\beta_2}}{C_{\beta_2}(1)}, \tag{17}$$

where $\beta \in (0, 2]$ is the jump activity index and k_n satisfies $(1/K \leq k_n \Delta_n^{\rho} \leq K)$ for $(0 < \rho < 1)$ and $(0 < K < \infty)$. In (17), $g(\cdot)$ is an auxiliary function that disentangles jumps from the diffusion component. As in Jing et al. (2012), we assume that this function $g(\cdot)$ satisfies

$$g(x) = \begin{cases} |x|^p & \text{if } |x| \leq 1, \\ 1 & \text{if } |x| > 1, \end{cases}$$

for an even integer $p > 2$ and $(x := |\Delta_j^n X| / \alpha \Delta_n^{\varpi})$. For the intensity estimator (17), the quantity $C_\beta(1) = 1$ for $g = 1_{\{x>1\}}$ and its general form can be given by

$$C_{\beta_2}(k_n) = \int_0^{\infty} (g(x))_n^k / x^{1+\beta_2} dx.$$

In sum, the estimates for the functional form $U(H)$ and jump intensity λ_t allow us to construct a test statistic to identify the mutual excitation across financial assets. This implies that we first need to estimate the spot jump intensities (via Equation (17)) and then use the estimates for calculating the measure in Equation (16). Armed with this setup, we present the main hypotheses and the corresponding testing procedures in the next section.

2.3. Hypotheses and testing procedures

Our identification approach for market linkages relies on mutual excitation dynamics. To characterize financial flights and market shock dependence, the first step is to test for the presence of cross-excitation in jumps. Let X_1 and X_2 denote asset 1 and asset 2, respectively. Empirically, we ask the following question: do jumps in asset X_1 (X_2) *excite* the jump occurrences in asset X_2 (X_1)? To answer this question, we consider the following testable hypotheses:

(A)	H_0: *No jump excitation from* X_1 *to* X_2	vs.	H_1: *Jump excitation from* X_1 *to* X_2
(B)	H_0: *No jump excitation from* X_2 *to* X_1	vs.	H_1: *Jump excitation from* X_2 *to* X_1
(C)	H_0: *Jump excitation from* X_1 *to* X_2	vs.	H_1: *No jump excitation from* X_1 *to* X_2
(D)	H_0: *Jump excitation from* X_2 *to* X_1	vs.	H_1: *No jump excitation from* X_2 *to* X_1

These hypotheses allow us to investigate not only the jump cascades across regions but also the *origins* of shocks. To proceed, let ω denote a specific outcome, i.e., $\omega \in \Omega$. Methodologically, we need to make an inference about ω, given a discretely observed sample path over $[0, T]$. The outcome could belong to the "no excitation set" ($\omega \in \Omega_T^{\text{no}}$) or to the "excitation set" ($\omega \in \Omega_T^{\text{mut}}$). We test **(A)**−**(D)** by comparing a test statistic to its probability limit under the alternative hypotheses. We first consider the null hypotheses of "no mutual excitation" (i.e., **(A)** and **(B)**).

Theorem 1. *Let* $\varpi \in (0, 1/2)$. *Suppose that Assumptions 1, 2, 3 (see Appendix A) hold with* $p > \frac{1-\varpi\beta_2}{1/2-\varpi}$, $q \geq 2$ *and* $q' \geq 1$, *and*

$$1 - \varpi\beta_2 < \rho < (1 - \varpi\beta_2) + 2\phi' \wedge 2\phi'' \wedge \frac{1}{2}\varpi\beta_2, \tag{18}$$

In addition, if either one of the following conditions is satisfied,

(a) $H(x_1, x_2, y_1, y_2) = 0$ *for* $|x_1 - x_2| \leq \epsilon$, *where* $\epsilon > 0$;

(b) $q' > 2$, $2\varpi\beta_1 < 1$ *and* $\rho < 1 - \varpi\beta_2 + 2\big((q'/2 - 1) \wedge \varpi(q \wedge q' - \beta_1)\big)$.

then, for any fixed $t > 0$, *under* H_0 *of* ***(A)***, *we have*

$$t_n^{12} := \sqrt{\frac{k_n\Delta_n}{\Delta_n^{\varpi\beta}}} \frac{U(H, k_n)_T^{12}}{\sqrt{U(G, k_n)_T^{12}}} \xrightarrow{\mathcal{L}_{st.}} \mathcal{N}(0, 1), \tag{19}$$

where $U(G, k_n)_T$ *is the consistent estimator of the conditional variance with*

$$G(x_1, x_2, y_1, y_2) = \frac{\alpha^\beta C_\beta(2)}{(C_\beta(1))^2}(y_1 H_3'(x_1, x_2, y_1, y_2)^2 + y_2 H_4'(x_1, x_2, y_1, y_2)^2), \tag{20}$$

where H_3' and H_4' stand for the first partial derivatives of the function $H(.)$ with respect to its 3rd and 4th arguments, respectively. $H(.)$ can be in the following form:

$$H(x_1, x_2, y_1, y_2) = |x_2 - x_1|^p \left(2 \cdot \log\left(\frac{y_1 + y_2}{2}\right) - \log(y_1) - \log(y_2)\right). \tag{21}$$

*However, under H_1 of **(A)**, we have $|t_n^{12}| \xrightarrow{\mathbb{P}} \infty$.*

Therefore, the following critical region has an asymptotic level α for testing the null hypothesis of "no mutual excitation" (i.e. Ω_T^{no}), and asymptotic power 1 for the alternative (i.e., Ω_T^{mut}):

$$C_n^{no} = \left\{t_n^{12} > z_\alpha\right\}, \tag{22}$$

where $\mathbb{P}(W > z_\alpha) = \alpha$ and W is a standard normal random variable.

Under the null hypothesis of "mutual excitation" (i.e., **(C)** and **(D)**), the asymptotic behavior of the test statistic is as follows.

Theorem 2. *Assume $P(\Omega_T^{(-)}) = 0$ and that the same assumptions as in Theorem 1 hold, but with (H-1) replaced by (H-2). In addition, assume H satisfies the following degenerate condition:*

$$y_1 = y_2 \Longrightarrow \|H_3'(x_1, x_2, y_1, y_2)\| + \|H_4'(x_1, x_2, y_1, y_2)\| = 0. \tag{23}$$

If either condition (a) or (b) in Theorem 1 is satisfied, then the following critical region has an asymptotic level α for testing the null hypothesis Ω_T^{mut}:

$$C_n^{mut} = \{|R_n| > z_\alpha \sqrt{V_n}\}, \tag{24}$$

where

$$R_n = \frac{U(H, wk_n)_T - U(H, k_n)_T}{U(H, k_n)_T} \quad \textit{and} \quad V_n = \frac{\Delta_n^{\varpi\beta}}{k_n \Delta_n} \frac{(w-1)U(G, k_n)_T}{w(U(H, k_n)_T)^2}. \tag{25}$$

Moreover, choose a sequence of positive numbers v_n such that

$$v_n \to 0, \quad \textit{and} \quad \frac{k_n v_n \Delta_n}{\Delta_n^{\varpi\beta}} \to \infty,$$

and set $V_n' = V_n \wedge v_n$. Then, the critical region

$$C_n'^{mut} = \{|R_n| > z_\alpha \sqrt{V_n'}\} \tag{26}$$

has an asymptotic level α for testing the null hypothesis Ω_T^{mut} and asymptotic power 1 for the alternative $\Omega_T^{(0)}$.

Therefore, we have two statistics to test for mutual excitation between jumps. Under the null hypothesis of no mutual excitation (i.e., **(A)** and **(B)**), we have the statistic in (19), and under the null hypothesis of excitation (i.e., **(C)** and **(D)**), we use the statistic in (26).

3. Monte Carlo study

Having presented our testing procedures and hypotheses, we now assess the finite sample properties of the test statistics. Throughout this section, we consider an observation length of one week and a sampling frequency of 5 seconds. We thus set $T = 5/252$ and $M = 23400$, giving $\Delta_n = 1/23400$. Following Aït-Sahalia and Jacod (2009) and Jing et al. (2012), we further choose the values $\varpi = 1/3$, $\rho = 0.6$ and $\beta = 1.25$. We conduct each simulation with 1000 replications.

3.1. Simulation setup

Our simulation setup is based on a bivariate Hawkes process with mutually exciting jumps. As in Aït-Sahalia et al. (2014) and Boswijk et al. (2014), we consider the following data-generating process:

$$\begin{cases} dX_{1,t} = \sigma_{1,t} dW_{1,t} + \lambda_{2,\infty} dY_{1,t} \\ dX_{2,t} = \sigma_{2,t} dW_{2,t} + \lambda_{2,t-} dY_{2,t} \\ d\sigma^2_{1,t} = d\sigma^2_{2,t} = \kappa(\theta_1 - \sigma^2_{1,t}) + \eta_1 \sigma_{1,t} dB_{1,t} \\ d\lambda_{2,t} = \kappa_\lambda(\lambda_{2,\infty} - \lambda_{2,t})dt + \eta_\lambda dB'_{2,t} + \xi \, 1_{\{|\Delta X_{1,t}| > \epsilon\}}. \end{cases}$$

where the Brownian motions ($W_{1,t}$, $W_{2,t}$, $B_{1,t}$, $B'_{2,t}$), and the β-stable jump processes ($Y_{1,t}$, $Y_{2,t}$) are assumed to be independent. We consider $\mathbb{E}\left[dW_{1,t} dB_t\right] = \phi dt$, which allows us to capture a potential leverage effect between prices and volatility dynamics. For the volatility process (third equation), we follow Jing et al. (2012) and set $\kappa = 5$, $\theta_1 = 1/16$, $\eta_1 = 0.5$ and $\phi = -0.5$. For the jump intensity process (fourth equation), we set $\kappa_\lambda = 1400$, $\eta_\lambda = 200$ and $\epsilon = 100\sqrt{\theta}\Delta_n^{\varpi}$ as in Boswijk et al. (2014). $\lambda_{2,\infty}$ further denotes the constant jump intensity, and we calibrate this value to generate pre-specified values of the tail probability for 0.25%. That is,

$$P(|\lambda_{2,\infty}\Delta_i^n Y_1| \geq \alpha\Delta_n^{\varpi}) \approx \frac{2c_\beta \lambda_{2,\infty}^{\beta} \Delta_n}{\beta(\alpha\Delta_n^{\varpi})^{\beta}}, \tag{27}$$

where

$$c_\beta = \frac{\Gamma(\beta+1)}{2\pi} \sin\left(\frac{\pi\beta}{2}\right). \tag{28}$$

We set $\alpha = 5\sqrt{\theta}$, and β denotes the jump activity index. With the choice of $\beta = 1.25$, the calibrated value for λ_∞ is approximately 20.[15]

The intuition behind our simulation setup is the following. When we set $\xi = 0$, there is no mutual excitation in jumps from one asset (X_1) to another (X_2). In this case, we can thus consider (i) a null hypothesis of no mutual excitation (i.e., **(A)**) or (ii) a null hypothesis of mutual excitation (i.e., **(C)**). For each null, we can check the size and power of the testing procedures. Similarly,

[15] In Section 5, we check the sensitivity of the test statistics to different β values. The results for $\beta = 1.5$ and $\beta = 1.75$ are rather similar.

when we set $\xi > 0$, jumps can excite as long as the price changes are large enough (i.e., when $|\Delta_n X_{1,t}| > \epsilon$). To choose the excitation parameter ξ, we utilize the following form

$$\frac{P(|(\lambda_{2,\infty} + \xi)\Delta_i^n Y_1| \geq \alpha \Delta_n^{\varpi})}{P(|\lambda_{2,\infty}\Delta_i^n Y_1| \geq \alpha \Delta_n^{\varpi})} \approx \left(\frac{\lambda_\infty + \xi}{\lambda_\infty}\right)^{\beta} = (1 + \xi/\lambda_\infty)^{\beta}. \tag{29}$$

For $\xi = 12$, the ratio in (29) is around 1.80. This implies that the mutual excitation effect will increase the tail probability by 80% (in relative terms), which is statistically and economically significant. Given this setup, the test statistic is given by

$$\mathcal{T} := \sqrt{\frac{k_n \Delta_n}{\Delta_n^{\varpi\beta}}} \frac{U(H, k_n)_T}{\sqrt{U(G, k_n)_T}} \begin{cases} \xrightarrow{\mathbb{P}} -\infty & \omega \in \Omega_T^{(-)}, \\ \longrightarrow \mathcal{N}(0,1) & \omega \in \Omega_T^{(0)}, \\ \xrightarrow{\mathbb{P}} +\infty & \omega \in \Omega_T^{(+)}, \end{cases}$$

where the function H takes the following form

$$H(p,q) = H(x_1, x_2, y_1, y_2; p, q) = |x_2 - x_1|^p \cdot (y_2 - y_1)^q \cdot 1_{\{|x_2 - x_1| \geq \epsilon\}}, \tag{30}$$

where $\epsilon > 0$ and—following Boswijk et al. (2014)—we consider two alternative functions for $H(p,q)$: $H(6,1)$ and $H(0,1)$. The next section reports the finite sample properties of our testing procedures.

3.2. Simulation results

To check the power and size properties, we consider four null hypotheses—presented in Section 2.3 (**(A)** to **(D)**). We proceed as follows. In the next section, we set the excitation parameter $\xi = 0$ in order to test for *no* mutual excitation in *all* directions, that is, either from X_1 to X_2 or from X_1 to X_2. In Section 3.2.2, we conduct simulations when $\xi = 12$ and test for the mutual excitation in jumps. In the final section, we adjust our simulation setup to test specifically for the *financial flights* from one asset to another.

3.2.1. Size and power properties: testing for no mutual excitation

We start by considering the null hypothesis **(A)** such that jumps in asset X_1 do *not* excite the jumps in asset X_2. Figure 3 shows the size and power of the tests for no mutual excitation in jumps. The solid line in the upper-left panel of the figure indicates that the size of the test is rather good. That is, when $\xi = 0$ (no excitation), the percentages of rejection, (i.e., $\mathcal{T} > z_\alpha$), are all close to their corresponding nominal level, α.

[Insert Figure 3 about here]

In a similar way, we further analyze the size of the test under the null hypothesis that X_2 jumps do *not* excite X_1 jumps (hypothesis **(B)**). The upper-right panel of Figure 3 shows that the test also exhibits a well-behaved size in this direction of jump transmission. The Monte Carlo rejections are close to the nominal level of the test at a 5-second sampling frequency.

We can examine the power of the test by considering the same excitation parameter $\xi = 0$. Intuitively, if there is no mutual excitation in jumps (i.e., $\xi = 0$), we should reject the null hypotheses of mutual excitations (corresponding to hypotheses **(C)** and **(D)**). The dotted (dashed-dotted) line in the upper-left (-right) panel of Figure 3 displays the power performance. Two results emerge from the panels. First, under the null hypothesis that jumps in X_1 excite the jumps in X_2 (hypothesis **(C)**), the power of the test is weak (dotted line). Second, if we consider a null hypothesis of (reverse) mutual excitation from X_2 to X_1 ((hypothesis **(D)**), then the test has good power (dashed-dotted line). This implies that—in the absence of mutual jump excitation in the data (i.e., $\xi = 0$)—we reject the null hypothesis of mutual excitation from X_2 to X_1.

3.2.2. Size and power properties: testing for mutual excitation

We now assess the size and power of our tests in the presence of mutual excitation between jumps. We set the excitation parameter as $\xi = 12$, which is a reasonable value implying that mutual excitation (originated in asset X_1) will increase the tail event likelihood (in X_2) by 80%. Figure 4 displays the size and power of the tests for mutual excitation in jumps.

[Insert Figure 4 about here]

The upper-left panel of Figure 4 (dotted line) shows that the test has good size under the null hypothesis that jumps in X_1 excite the jumps in X_2 (i.e., hypothesis **(C)**). Put differently, if there are jumps in the data, we do not reject the null hypothesis of jump excitation from X_1 to X_2. The percentages of rejection in simulations are close to the corresponding nominal level α.

The upper-left panel of Figure 4 (solid-line) further indicates that the power of our test is quite reasonable. That is, in the presence of mutual excitation, if we consider the null hypothesis that there is *no* mutual excitation from X_1 to X_2 (hypothesis **(A)**), we reject this null hypothesis in simulations.

With the choice of $\xi = 12$ (presence of mutual excitation), we plot in Figure 4 (upper-right panel) the size and power performance of our test. We now consider the null hypothesis that jumps in X_2 do *not* excite the jumps in X_1 (hypothesis **(B)**). The percentages of rejection in the figure depict a forty-five-degree (dashed) line, indicating a well-behaved size. This result is consistent with the size performance when the null hypothesis is an excitation from X_1 to X_2. In other words, if there is an excitation from X_1 to X_2 (accepting hypothesis **(C)**), we should also accept the null hypothesis that X_2 jumps do not excite X_1 jumps (hypothesis **(B)**). Our test statistic identifies these two properties.

[Insert Figures 5 and 6 about here]

Lastly, we consider hypothesis (**(D)**), which states that jumps in X_2 excite jumps in X_1. The upper-right panel of Figure 4 shows (dashed-dotted line) that the power of the test—under this null—is quite strong. This result is expected because if the test has good size under the null hypothesis (**(C)**), then it should be powerful to reject the null hypothesis (**(D)**). As the lower panels of Figures 3 and 4 indicate, the size and power properties of the testing procedures are

robust to different specifications of the functional form $H(p,q)$—in Equation (30)—of the test statistic (i.e., $H(0,1)$ vs. $H(6,1)$). Moreover, while sampling at a lower frequency (e.g., 1 minute) deteriorates the power, its impact on size remains limited (see, e.g., the upper panels in Figures 5 and 6).[16]

3.2.3. An alternative specification: testing for financial flights

It is important to note that mutual excitation from one asset (X_1) to another (X_2) does not necessarily imply a "financial flight". In particular, a flight-to-safety episode occurs when a large *negative* return (or jump) in one asset (e.g., stocks) coincides with a large positive return (or jump) in the other asset (e.g., bonds). We are now interested in checking the size and power of our tests by simulating financial flights. To do so, we slightly modify our simulation (DGP) setup and consider a case where the jump intensity of asset X_2 increases only with negative jumps in asset X_2. Figure 7 displays the size and power of our tests for financial flights between two assets. We report the main results in three cases.

[Insert Figure 7 about here]

Case I (flight from X_1 to X_2). This is the case of a *flight to safety* (FTS) episode. We consider a null hypothesis that negative jumps in asset X_1 increase (positive) jump intensity in asset X_2. Under this null hypothesis and with the choice of $\xi = 12$, the left (first and second) panels of Figure 7 show that the size of the test is quite good (dotted lines). For the null hypothesis of *no* flight from X_1 to X_2, the testing power is reasonable but not very strong (solid lines).

Case II (flight from X_2 to X_1). This case corresponds to a *seeking returns strategy* (SRS) episode when we consider X_1 and X_2 as the risky and safe-haven assets, respectively. The right (first and second) panels of Figure 7 display the simulation results. For the null hypothesis that there is no financial flight from X_2 to X_1 (dashed line), the size of the test is rather good. Intuitively, this finding is also consistent with the results under *Case I* such that if there is a flight from X_1 to X_2, we should not simultaneously observe a (reverse) flight from X_2 to X_1.

Case III (financial flight when the news is good). In practice, FTS episodes occur due to negative news events or surprises. That is, when the bad news hits the market, investors tend to sell off risky assets (such as stocks) and shortly invest in safe assets (such as U.S. Treasury bonds). Nevertheless, if the news is good news, then both assets might exhibit positive jumps: the intensity of jumps in one asset (i.e., X_2) can increase with positive jumps in the other asset (i.e., X_1).

We now focus on this possibility and test for mutual excitation (or flight) only when positive jumps propagate. The two lower-row panels of Figure 7 demonstrate that our testing procedure is capable of capturing such patterns in the simulated data. Under the null hypothesis that only positive jumps are mutually exciting, the test delivers a good-size performance (left panels, third

[16] The results using a 5-minute frequency are qualitatively similar.

and fourth rows). Similarly, if we consider a null hypothesis of no positive jump excitation (from X_2 to X_1), we do not reject this hypothesis (right panels, third and fourth rows). Power properties are not strong, particularly under the null hypothesis of no excitation, but relatively reasonable when the excitation direction is from X_2 to X_1 (dashed-dotted lines in lower-left panels).

4. Empirical analysis

In this section, we study the dynamics of financial flights and stock market linkages revealed by our excitation tests. After describing the database, we present and discuss our empirical findings.

4.1. Data

We use 5-minute data for the S&P 500 stock index, 30-year U.S. Treasury bond futures, gold futures and MSCI emerging market indices (global/Asia/Latin America). The data span January 1, 2007 to December 31, 2013. Thompson Reuters provides transaction prices throughout the trading days for each asset class.[17]

As is typical in the literature, we omit trading days with too many missing values or low trading activity.[18] Similarly, we delete weekends, certain fixed/irregular holidays, empty intervals and consecutive prices.[19] We further adjust the financial market data according to daylight savings time, considering the (trading) time zones of the assets. Appendix B presents the details of the data descriptions and our adjustment procedures.

4.2. Flights to safety episodes: mutual excitation from the U.S. stock market to the gold market

We begin by identifying flight to safety (FTS) episodes occurring between S&P 500 index and gold prices. Specifically, we capture FTS patterns by testing for the mutual excitation from (negative) jumps in the market index to (positive) jumps in gold prices. To implement this analysis, we consider four categories.

The first category (Cat.1) is the case in which we reject the null hypothesis of no mutual excitation and accept the null of mutual excitation jointly. Therefore, the FTS events fitting this category reveal evidence of cross excitation from S&P 500 to gold prices. In the second category (Cat.2), we search for the periods in which there is no FTS through mutual excitation test. This category hence relies on a situation in which (i) we accept the null hypothesis of no mutual excitation and (ii) reject the null of mutual excitation. Lastly, we characterize the episodes in which we cannot accept or reject the null hypothesis. The jump-type financial shocks associated with these categories (Cat.3 and Cat.4) do not propagate across assets.

[17] The raw bond futures and stock index datasets include all open-close, high-low prices. In our empirical analysis, we use closing prices.

[18] See, e.g., Dewachter et al. (2014), Lahaye et al. (2011).

[19] These holidays include the New Year (December 31 - January 2), Martin Luther King Day, Washington's Birthday or Presidents' Day, Good Friday, Easter Monday, Memorial Day, Independence Day, Labor Day, Thanksgiving Day and Christmas (December 24 - 26).

[Insert Table 2 about here]

As in Baele et al. (2014), we study financial flights in various forms depending on the strength of tail shocks: weak, mild and severe. In our analysis, we control the FTS levels by considering different jump sizes. Moreover, we account for the impact of stochastic volatility by choosing threshold values when testing for flights. While lower thresholds tend to increase jump activity or frequency (see, e.g., Todorov and Tauchen, 2010), high threshold values allow us to analyze propagation between large/infrequent jumps.

Based on these criteria, Table 2 reports the frequency (in %) of FTS episodes falling into each category from Cat.1 to Cat.4. For the Cat.1 with $\alpha = 2$, the table presents evidence of mutual excitation between jumps in S&P 500 and gold prices (fourth column); 25−30% of all common jump arrivals are in the form of financial flights from stocks to gold (first row in the fourth column). The table also indicates that the frequency of FTS trades increases with jump sizes (third column). For instance, when financial shocks are weak (corresponding to size 0.001), FTS variation in the data is around 18%. The FTS activity surges substantially to 41% when jump shocks hitting the markets are relatively severe (corresponding to size 0.009). This result supports the conclusion of Boswijk et al. (2014), in the sense that extreme (jump) events are more likely to trigger mutual excitation, which, in turn, causes investors to sell off risky assets and invest in safe havens.

The fifth column of Table 2 further shows that the evidence of mutual excitation weakens as the volatility thresholds increase, e.g., from $\alpha = 2$ to $\alpha = 5$. For instance, with the choice of $\alpha = 2$, 8% of periods do not exhibit FTS trades (Cat.2), whereas there is no strong evidence of mutual excitation for $\alpha = 3$ (11%) and $\alpha = 5$ (15%). Categories 3 and 4 finally report the percentage of periods with *indeterminate* FTS regions. While rejecting both null hypotheses is not likely (3−11% in the sixth column), there are many periods in which our testing procedures accept both null hypotheses for excitation effects (50−75% in the sixth column). As Baele et al. (2014) argue, one explanation for this finding could be that when systematic and idiosyncratic jumps occur jointly within the same periods, mutual excitation occurs and, hence, financial flights become intractable. We observe such regularities in the jumps of S&P 500 index and gold prices.

[Insert Table 3 about here]

Given the presence of mutual excitation, we are now interested in timing the arrivals of financial flights between stocks and gold. Using our mutual excitation tests, we proceed in two ways. First, we identify the FTS periods in which we observe flows from equities to the gold market. These FTS episodes represent *risk-off* trading schemes. Second, we consider the regimes of *risk-on* trades, which implies a (reverse) financial flight from safe havens to risky assets (i.e., from gold to stocks). We call this trading mechanism the *seeking-returns-strategy* (SRS). Intuitively, while FTS episodes capture the market conditions in which investors increase their holdings in safe assets, SRS regimes reflect the periods when risk appetite surges in the marketplace. Table 3 presents the (business cycle) periods of flight-to-safety (FTS) and seeking-returns-strategy (SRS) identified by the mutual excitation tests.

The table indicates that, over the sample years 2007-2014, the second and third quarters of 2007 are distinct FTS states (columns 2 and 4). The identified jump excitation spells surround the beginning of the liquidity crisis when BNP Paribas froze the redemption for three investment funds on August 9, 2007. The data exhibit FTS patterns even in the last quarter of 2007 (column 5), reflecting the persistence of market fear and stress. Negative (jump-type) shocks hitting stock markets excite positive jumps in commodities.

Furthermore, while the first half of 2008 contains neither FTS nor SRS periods (rows 2008/Q1 and 2008/Q2), the third quarter (July-September 2008) is linked solely to FTS regimes. One explanation for this result could be related to investors' judgment about tail risk events. The events tied to the bankruptcy of Bear Stearns (mid-March 2008) did not significantly lead to risk-off flights from U.S. stocks to safe assets. The collapse of Lehman Brothers, however, appears to create severe FTS spells (row 2008/Q3) with high degrees of mutual excitation between equities and gold (i.e., $\alpha = 5$). For the periods following 2009, Table 3 shows the clusters of FTS and SRS regimes at different strength levels ($\alpha = 2, 5$). For example, while the first quarter of 2009 can be characterized as an SRS cycle, the last quarter of 2009 contains FTS regimes. The table reveals similar FTS/SRS regularities until the end of 2012. Regardless of the choice of flight level (i.e., either $\alpha = 5$ or $\alpha = 2$), we do not find strong evidence of financial flights in 2013.

4.3. Flights to quality episodes: cross-excitation between stocks and bonds

The previous section identifies flight-to-safety episodes—between stocks and gold—based on the mutual excitation tests. In this section, we analyze the excitation dynamics in U.S. capital markets, and instead characterize flight-to-quality (FTQ) spells propagating from stocks to bonds. Similar to our FTS analysis, we begin by testing for mutual excitation between negative jumps in the stock prices and positive jumps in the bond prices. Table 4 reports the test results for the S&P 500 index and long-term (30-year) U.S. treasury bond futures.

[Insert Table 4 about here]

In approximately one-fifth of quarters, we observe flights from the U.S. stock market to the bond market (column 4 in the first panel). The frequency of FTQ regimes significantly diminishes as jump variation dominates volatility (i.e., in the fourth column from $\alpha = 2$ to $\alpha = 5$). For the 2007-2014 sample, only approximately 10% of periods contain FTQ trades with the choice of $\alpha = 3$. Larger jump thresholds (e.g., $\alpha = 5$) indicate the absence of mutual excitation between S&P 500 and 30-year bond futures. Overall, these results imply that FTQ occurs mostly (I) when the flight level is weak (i.e., for smaller jump size) and (II) when volatility dominates jumps (i.e., for lower α).

We now turn to answer the following question: when do FTQ cycles occur and how frequent are they compared to FTS events? Table 5 presents the arrival times of the detected FTQ spells together with the SRS episodes. To ease the interpretation of the findings, we compare the FTQ occurrences with the identified FTS regimes provided by Table 3. Overall, several results emerge

from those tables. First, FTQ occurs less frequently than FTS over the entire sample period 2007−2013 (left panels in Tables 5 and 3, respectively). The evidence is more pronounced with larger levels of α, that is, when jump shocks become more severe relative to stochastic volatility. For instance, while we pin down 5 FTS quarters (over 27) at the $\alpha = 5$ level, there is only 1 FTQ episode based on the same flight level (second columns, Tables 3−5, respectively).

[Insert Table 5 about here]

Second, although we can consider both FTQ and FTS as *escape strategies* from risk, they occur in different financial cycles. For example, Table 5 indicates the absence of any FTQ trades between 2007/Q4-2010/Q1. On the contrary, the excitation tests characterize two distinct FTS periods (i.e., 2008/Q3, 2009/Q4) within the same sample range. This may suggest that during the period of Lehman Brothers' collapse (2008/Q3), investors appear to have sold off stocks and fled to safety (i.e., gold) rather than quality (i.e., bonds). Furthermore, as the left panel of Table 3 reveals (row 2008/Q3), these results hold regardless of the level of flight (i.e., α) and functional choice for the excitation test (FTS (1) or FTS (2)).

Third, SRS exhibits *asymmetric* patterns linked to FTS and FTQ trades. Specifically, comparing the right panels of Table 3 with those in Table 5, we observe that SRS from safe havens occurs more frequently than SRS from bond investments, especially if the jump threshold is high ($\alpha = 5$). That is, when large adverse shocks hit financial markets, investors tend to move away from risk towards safety of gold and quality of bonds (i.e, FTS and FTQ spells, respectively). Our results suggest that, as the market jump turmoil settles down, traders typically move back to risky assets (i.e. stocks) by mostly selling gold rather than long-term U.S. debt. While negative jumps in gold prices *excite* positive jumps in the S&P 500 index, evidence of a reverse excitation effect—from bonds to stocks—is considerably weak.

4.4. International flights: stock market linkages in the global financial system

In the previous section, we presented evidence of mutual excitation in the form of financial flights (FTS and FTQ). Relying on our excitation tests, we are now interested in characterizing the global stock market linkages, particularly between U.S and emerging markets. For this, we proceed as follows. First, we test for the presence of cross-excitation effects. Specifically, we identify the frequency, arrival times, and direction of mutual excitation patterns in the data. Second, we decompose the emerging markets into two sub-regions, Asian and Latin American countries, which allows us to better identify the source of adverse events that propagate to the U.S.

[Insert Table 6 about here]

Table 6 reports the results of the mutual excitation tests. As in our previous analysis, we measure the market excitation at different levels: low-to-high jump variation thresholds (i.e., α from 2 to 5) and shock sizes (i.e., from 0.001 to 0.009). The first category of results (column MI Cat.1) provides evidence of cross-excitation from emerging markets to the U.S. The table indicates

that around 20% of periods over the sample are associated with mutually exciting jumps (fourth column). While the results remain the same with different jump cutoffs (i.e., α), there is no evidence of jump excitation if the adverse shocks are severe (from 0.001 to 0.009). The second category of results (MI Cat.2) reinforces this finding. Emerging market jumps with very large sizes (e.g., 0.009) do not appear to increase the likelihood of (future) shocks in the U.S. Except with the choice of $\alpha = 5$, approximately one-half of all periods exhibit no excitation linkage between severe jumps (i.e., 0.009). Moreover, as the bottom-right corner of Table 6 shows, the statistical evidence is inconclusive (100%) when we choose high jump cutoffs ($\alpha = 5$) and sizes (0.009).

[Insert Table 7 about here]

We now consider the reverse transmission of jump excitation flowing from the U.S. to emerging markets. Table 7 presents the test results under different categories, ranging from the excitation region (Cat.1) to inconclusive regions (Cat.4). The most striking finding here is that the excitation channel is *asymmetric*. In sharp contrast to the results in Table 6, the third column of the table (Cat.1) provides little evidence of mutual excitation from the S&P 500 to the MSCI index. With the choice of $\alpha = 2$, the percentage of periods including cross-excitation is only approximately 4%. This evidence remains weak even if jump threshold increases from $\alpha = 2$ to $\alpha = 4$. For higher degrees of shock (i.e., with jump sizes from 0.001 to 0.009), the tests slightly indicate the presence of excitation (8%) as long as the jump variation strongly dominates ($\alpha = 5$). Given the results in the bottom row of Table 7, evidence of excitation is rather mixed, and 70% of periods do not comprise excitation effects.

[Insert Table 8 about here]

These findings support the view of Glick and Hutchison (2013), who show that transmission of U.S. equity returns to Asian markets is considerably weak, especially during the 2008−2009 period. We confirm this conclusion through jump spillovers and excitation effects. Specifically, comparing the results in Table 6 with those reported in Table 7, we show that jumps in emerging market equity returns tend to propagate to the U.S. equity market, not the reverse. These results, however, differ from Aït-Sahalia et al. (2014), who document that U.S. market jumps have more influence on jump shocks in other markets. The differences between the results could be due to several reasons. First, unlike Aït-Sahalia et al. (2014), we are particularly interested in measuring the excitation effects between U.S. and emerging markets, leaving other markets aside. Second, we use high-frequency data to test for the mutual excitation across regions, instead of daily data, as in Aït-Sahalia et al. (2014). This could partly explain the additional information content embedded in intraday dynamics to explain excitation effects. Third, while we focus on relatively recent market conditions (2007−2013), the data sample of Aït-Sahalia et al. (2014) spans 1980−2012. We test for the presence of cross-excitation in a nonparametric way, whereas the empirical approach of Aït-Sahalia et al. (2014) is parametric, relying on GMM-based estimation procedures. Last but not least, the direction and magnitude of chain reactions may change over time due to the characteristics

of the source of the turmoil in the markets. Kaminsky et al. (2003) call these linkages *fast and furious* contagion. For instance, a severe jump-type tail event originating in emerging markets may affect the hub countries (such as U.S.), which, in turn, influences the other developed countries and/or emerging markets. The empirical challenge is then to pin down the periods of propagation. Based on this intuition, our analysis tracks the shock transmission episodes that help to accurately assess the times of the directional shifts.

[Insert Table 9 about here]

To characterize the transmission of jump-type shocks, we present in Table 8 the direction and frequency of excitation episodes. The table confirms the previous finding for the excitation channel: the shocks occurring in emerging markets tend to create a higher impact on the U.S. than the reverse (left and right panels, respectively). While, surprisingly, the right panels indicate almost no evidence of excitation (from S&P 500 to MSCI), the left panels contain several periods of market stress. The first and second sets of those episodes occur around the third quarters of 2007 and 2008. These periods are associated with, for instance, the liquidity case of BNP Paribas (2007/Q3), the bankruptcy of Lehman Brothers, the rescue of AIG, and the subsequent implementation of the Trouble Assets Relief Program (2008/Q3−2008/Q4). The third set of linkages occurs mostly in the second and third quarters of 2011 and 2012, in which the European debt crisis intensified (left panel of Table 8). More broadly, these results are in line with Alexeev et al. (2015) in the sense that market risk dynamics change substantially during turbulent periods. Related to our findings, this notion could further explain the absence of excitation in jumps from U.S. to emerging markets. High volatility in the U.S. market appears to diminish the influence of strong jump transmission across geographic regions.

Finally, given the evidence that MSCI jumps excite S&P 500 jumps, we examine which particular geographic region generates the excitation effects. Table 9 reports the test results by splitting the MSCI emerging markets into two main categories: Asian (Panel A) and Latin American countries (Panel B). For brevity, we consider two jump cutoff values $\alpha = 2$ and $\alpha = 5$. The fourth column of the table (Cat.1) reveals that U.S. market appears to be more vulnerable to jump-type shocks from Latin American countries relative to Asian markets. For instance, with the choice of $\alpha = 2$, approximately 10-14% of the quarters contain Asia-driven excitation effects, whereas market linkages from Latin America to the U.S. are stronger (25-30%) over the entire sample (2007−2013). For both regions, the frequency of jump transmission decreases as the shock thresholds increase (i.e., from $\alpha = 2$ to $\alpha = 5$). The table further suggests that these results remain qualitatively similar as we consider different magnitudes of jump linkages (e.g., 0.001, 0.009).

4.5. The mutual excitation between market volatility and price jumps

The previous sections documented the presence of mutual excitation across jumps in asset prices: when adverse shocks hit the markets, the data exhibit financial flights from stocks to commodities and U.S. long-term debt. In addition to these patterns, jumps propagate from one region to another, for instance, from emerging markets to U.S. equities.

Given this evidence, we now proceed by testing for the excitation effects between market-wise volatility and asset price jumps. Our analysis is particularly guided by the studies of Jacod and Todorov (2010) and Todorov and Tauchen (2011). While the former study derives a testing procedure to identify the co-jumps between volatility and prices, the latter provides empirical evidence that market volatility and asset prices jump mostly together. Understanding the link between market volatility and jump dynamics is important, especially for derivative pricing (Liu and Pan, 2003), risk premium estimation (Maheu et al., 2013; Todorov, 2010) and tail risk analysis (Bollerslev and Todorov, 2011).

We extend these studies by investigating a potential excitation channel between volatility jumps and price jumps. To test for the presence of excitation, we consider two null hypotheses. First, we test the hypothesis that price jumps do not excite volatility jumps. The second null hypothesis states the reverse direction: volatility jumps do not excite price jumps. As in Jacod and Todorov (2010), Todorov and Tauchen (2011), we use the VIX for the market volatility proxy and the S&P 500 for the underlying price index. For negative (left-tail) and positive (right-tail) jumps separately, Table 10 reports the frequency of periods for which we reject the each null hypothesis.

[Insert Table 10 about here]

Panel A of the table (Cat.1) indicates a strong mutual excitation from negative price jumps to volatility jumps (35% of periods). Consistent with the conclusions of Todorov and Tauchen (2011) and Aït-Sahalia et al. (2013), this result reveals evidence of a *leverage effect*: there is a negative correlation between asset returns and their changes in volatility. The proportion of periods with no excitation is only approximately 7% (Cat.2 in Panel A).

Panel B of the table (Cat.1) further shows that the evidence of excitation—from positive jumps to volatility jumps—is quite weak (3% of periods). This result is not surprising in view of the intuition that only downside (or negative) jump risk fuels market fear, and the impact of positive return jumps on market stress is rather limited.

Finally, Panel C of Table 10 presents the test results for reverse excitation from VIX jumps to S&P 500 jumps. The data exhibit a strong excitation effect from volatility to jumps. Approximately 33% of periods in the entire sample coincide with episodes in which volatility jumps lead to price jumps. One explanation for this finding could be related to the risk perception in the marketplace. When asset prices move with unusual jump events, investors expect market volatility to rise and, hence, protect themselves by demanding risk premia. The information flow in turn creates a feedback mechanism—an excitation channel—from volatility to asset prices. Jump fear embedded in market volatility increases the likelihood of jump cascades in financial markets.

5. Robustness checks and extensions

We assess the robustness of our results in several respects. First, we account for the impact of intraday periodicity in volatility. To achieve this, we filter out the periodic component of spot volatility from the data and apply our testing procedures to filtered log-returns. Second, we analyze

in simulations whether market microsructure noise impairs our testing procedures. Third, we investigate the choice of parameter values in affecting the size and power of the excitation tests. For brevity, we report only the main findings here.[20]

5.1. The impact of intraday periodicity

In the presence of periodicity, the distributional characteristics of filtered returns (Figure 8) and unfiltered returns (Figure 9) remain qualitatively similar.[21] As we apply our testing procedures on filtered returns, intraday periodicity appears to increase the number of episodes of indeterminate region (Cat.4), whereas its impact on the null hypothesis of excitation (Cat.1) is limited. For instance, we find that the frequency of FTS episodes becomes 12.50% (14.81%) with filtered (unfiltered) returns with the choice of $\alpha = 4$ and weak FTS level (0.001). For a given shock magnitude (e.g., $\alpha = 2$), results with periodicity-filtered returns are quite similar to those with our former results; the frequency of FTS flows increases with jump size.

[Insert Figures 8 and 9 about here]

Considering FTQ trades, we find that the impact of periodic volatility on identified frequencies remains limited. Perhaps surprisingly, periodicity-filtered tests indicate even stronger evidence of FTQ regimes in the data. The test results for stock market linkages are similar to those for FTS episodes. While periodic volatility barely affects (Cat.1) type results, joint-hypothesis tests (i.e., Cat.4) reveal mixed evidence. Overall, our main conclusions remain unchanged, and the impact of periodicity on our testing procedures is negligible.

5.2. The impact of market microstructure noise

Having analyzed the role of intraday periodicity, we now assess the effect of market microstructure noise on our mutual excitation tests. In the presence of noise, the true value of the log price is $X(d,t)$ (for assets $d = 1, 2$), as in Equation (1), but in the data, we observe $Z(d,t)$. That is (in differential form),

$$dZ_{d,t} = dX_{d,t} + de_{d,t},$$

where $e(t)$ is the additive noise term for each asset $d = 1, 2$. To calibrate the noise parameters, we follow Aït-Sahalia et al. (2012) and set $e_{d,t} = C\sigma_{d,t}\Delta^{1/2}\epsilon_{d,t}$ with $\epsilon_{d,t} \sim \mathcal{N}(0,1)$, and $C = 2, 6$ is the noise size. While this setup allows for temporal heteroscedasticity in noise, we also consider a case in which noise is independent of stochastic volatility (i.e., $e_{d,t} = C\epsilon_{d,t}$). Given this noise specification, we repeat our simulations in Section 3 to evaluate the performance of the tests in noisy high-frequency data.

[20] Our results are available upon request.

[21] To account for periodicity, we standardize raw returns ($r_{t,i}$) by intraday periodicity estimates ($\hat{f}_{t,i}$), i.e., $r^*_{t,i} = r_{t,i}/\hat{f}_{t,i}$, where $\hat{f}_{t,i}$ estimates the periodic component of the volatility. As in Boudt et al. (2011), we use the WSD estimator to filter out periodic components of volatility from the data. The procedures are available upon request.

When we consider temporal heteroscedasticity in noise, the simulations indicate that the tests are still correctly sized and powerful with the choice of $C = 2$.[22] As we increase the noise strength (from $C = 2$ to $C = 6$), empirical size remains unaffected, but we observe a small loss of power when testing for mutual excitation from asset X_2 to X_1. These results hold both in the absence (i.e., $\xi = 0$) and presence (i.e., $\xi = 12$) of excitation effects in simulations.

We next consider the case of *non-shrinking* noise such that noise is homoscedastic and independent of spot volatility. Under this noise specification, our results reveal that the impact of noise is non-negligible. Regardless of the noise size, we find that the tests become undersized and lose their power. Specifically, we notice that the Monte Carlo rejection frequencies are substantially lower than the corresponding theoretical levels, which generates almost flat lines in rejection figures instead of forty-five-degree lines (see e.g., Figure 4). While we do not develop noise-free excitation tests here, future research can remove noise from data by using the pre-averaging method of Aït-Sahalia et al. (2012).

5.3. Sensitivity of the tests to parameter values

We turn to the sensitivity analysis of the tests for different parameter values. Figure 10 displays the Monte Carlo rejection frequencies, and Table 11 reports the set of parameters chosen in each sensitivity analysis (from I to VI).

[Insert Figure 10 and Table 11 about here]

We begin by varying the idiosyncratic tail probability (sensitivity analysis I and II). As we increase the probability of observing a tail event (from 0.25% to 1% and 5%), the upper panels of Figure 10 indicate a small size distortion (dotted lines). Despite this result, we notice that the power of the test is quite strong for high values of tail probabilities (solid lines). We clearly reject the null hypothesis of no mutual excitation from X_1 to X_2.

In the second part of our sensitivity analysis, we set the tail parameter to 0.25% but increase the excitation likelihood from 80% to 90% and 99% (sensitivity analysis III and IV in Table 11, respectively). For these values, the excitation parameter ξ equals to 14 and 15 instead of 12 (i.e., the base parameter). The middle panels of Figure 10 show that the test is correctly sized (forty-five-degree dotted line) and the power is reasonable (solid line). The mutual excitation tests are considerably immune to the choice of excitation parameters.

Finally, we check the behavior of the tests when the jump activity is relatively high (lower panels of Figure 10). For this, we consider two β values and set $\beta = 1.50$ and $\beta = 1.75$ (V and VI in Table 11). In this case, we observe that the power remains unaffected (solid line), whereas the test is slightly undersized (dotted line). We summarize the main findings in the last two columns of Table 11: the behavior of excitation tests is quite good with the base parameters (see e.g., Section 3.2.2), and the tests are mostly insensitive to parameter choices.

[22] For brevity, we do not report the results. The figures showing the size and power of the tests are available upon request.

6. Conclusion

This paper examines the spillover effects of tail-type sudden shocks in global financial markets. Measuring linkages is empirically challenging because shocks are typically unobservable, clustered in a specific time period and subsequently likely to spread across different asset classes or borders. In times of crisis, correlation measures tend to be biased, posing further difficulties in understanding how (and when) markets are connected.

We develop an alternative approach to identify financial contagion in high-frequency financial data. This approach tracks the *time-variation*, *direction* and *strength* of different shock spillovers across assets and regions. In our specification, jump-type events in one asset have the potential to increase the intensity of further jumps in other assets, creating *mutual-excitation* effects. We propose a new nonparametric testing procedure that allows us to characterize the episodes of mutually exciting shock dynamics.

Using our proposed methodology, we study *jump linkages* in the form of stock market integration and financial flights, including FTS and FTQ. We find evidence of *cross-excitation effects*, particularly from emerging stock markets to the U.S., rather than the other way around. Perhaps surprisingly, the U.S. stock market appears to be quite resilient to shocks hitting Asian emerging countries and relatively more vulnerable to extreme events occurring in Latin American markets. This evidence supports the conclusion by Bae et al. (2003) but contrasts the findings by Aït-Sahalia et al. (2014). The use of intraday data therefore seems to be critical in terms of uncovering linkages between international stock markets.

Our analysis reveals two distinct features of financial flights. First, when risk aversion grips markets, investors demand both safety (gold) and quality (bonds), but they do so in different business cycles and for different shock levels. Second, as market fear and panic subside, risk appetite prompts investors to rebalance their portfolios toward stocks, particularly by selling gold rather than bonds. We reach this conclusion because, while large negative drops in gold prices result in positive jumps in the S&P 500, excitation from bonds to stocks turns out to be weak.

Using the mutual-excitation approach, we also show that past volatility (VIX) jumps increase the intensity of future price (S&P 500) jumps, providing evidence of *volatility feedback effects*. In the literature, studies typically consider news announcements and microstructure factors as determinants of (co)jump dynamics. New information and trading activity, however, can only partially explain the arrivals of (co)jumps in the data. Our results offer a potential resolution to this conflicting issue. In the presence of volatility feedback, fear proxies and market sentiments could be additional jump drivers, and *ex ante* measures of risk premium might explain the *ex post* variation in price discontinuities. This consideration may help improve the forecasting of extreme jump-type tail events and has important implications for asset pricing and risk management strategies.

References

Aït-Sahalia, Y., Cacho-Diaz, J., Laeven, R.J.A., 2014. Modeling financial contagion using mutually exciting jump processes. Forthcoming in Journal of Financial Economics.

Aït-Sahalia, Y., Fan, J., Laeven, R.J., Wang, C.D., Yang, X., 2014a. Estimation of the continuous and discontinuous leverage effects. Working Paper.

Aït-Sahalia, Y., Fan, J., Li, Y., 2013. The leverage effect puzzle: Disentangling sources of bias at high frequency. Journal of Financial Economics 109, 224–249.

Aït-Sahalia, Y., Hurd, T.R., 2016. Portfolio choice in markets with contagion. Journal of Financial Econometrics 1, 1–24.

Aït-Sahalia, Y., Jacod, J., 2009. Estimating the degree of activity of jumps in high-frequency data. Annals of Statistics 37, 2202–2244.

Aït-Sahalia, Y., Jacod, J., 2012. Analyzing the spectrum of asset returns: Jump and volatility components in high frequency data. Journal of Economic Literature 50, 1007–1050.

Aït-Sahalia, Y., Jacod, J., Li, J., 2012. Testing for jumps in noisy high frequency data. Journal of Econometrics 168, 202–222.

Aït-Sahalia, Y., Laeven, R.J., Pelizzon, L., 2014b. Mutual excitation in Eurozone sovereign CDS. Journal of Econometrics 183, 151–167.

Alexeev, V., Dungey, M., Yao, W., 2015. Time-varying continuous and jump betas: The role of firm characteristics and periods of stress. Working Paper.

Allen, F., Gale, D., 2000. Financial contagion. Journal of Political Economy 108, 1–33.

Andersen, T.G., Bollerslev, T., Diebold, F.X., Vega, C., 2007. Real-time price discovery in stock, bond and foreign exchange markets. Journal of International Economics 73, 251–77.

Bae, K., Karolyi, G.A., Stulz, R.M., 2003. A new approach to measuring financial contagion. Review of Financial Studies 16, 717–763.

Baele, E., Bekaert, G., Inghelbrecht, K. Wei, M., 2014. Flights to safety. National Bank of Belgium Working Paper No. 230.

Baele, L., Bekaert, G., Inghelbrecht, K., 2010. The determinants of stock and bond return comovements. Review of Financial Studies 23, 2374–2428.

Bansal, N., Connolly, R.A., Stivers, C., 2014. The stock-bond return relation, the term structures slope, and asset-class risk dynamics. Journal of Financial and Quantitative Analysis 49, 699–724.

Baur, D., 2012. Financial contagion and the real economy. Journal of Banking and Finance 36, 2680–2692.

Beber, A., Brandt, M.W., Kavajecz, K.A., 2009. Flight-to-quality or flight-to-liquidity? evidence from Euro-area bond market. Review of Financial Studies 22, 925–957.

Bekaert, G., Harvey, C.R., 1995. Time-varying world market integration. Journal of Finance 50, 403–444.

Bekaert, G., Harvey, C.R., 1997. Emerging equity market volatility. Journal of Financial Economics 43, 29–77.

Bekaert, G., Harvey, C.R., 2000. Foreign speculators and emerging equity markets. Journal of Finance 55, 565–614.

Bekaert, G., Harvey, C.R., Ng, A., 2005. Market integration and contagion. Journal of Business 78, 39–69.

Bibinger, T., Linzert, T., Winkelmann, L., 2015. ECB monetary policy surprises: identification through cojumps in interest rates. Forthcoming in Journal of Applied Econometrics.

Bibinger, T., Winkelmann, L., 2015. Econometrics of cojumps in high-frequency data with noise. Journal of Econometrics 184, 361–378.

Bollerslev, T., Law, T., Tauchen, G., 2008. Risk, jumps, and diversification. Journal of Econometrics 144, 234–256.

Bollerslev, T., Todorov, V., 2011. Tails, fears and risk premia. Journal of Finance 66, 2165–2211.

Boswijk, H.P., Laeven, R.J.A., Yang, X., 2014. Testing for self-excitation in jumps. Working Paper, University of Amsterdam.

Boudt, K., Croux, C., Laurent, S., 2011. Robust estimation of intraweek periodicity in volatility and jump detection. Journal of Empirical Finance 18, 353–367.

Brunnermeier, M.K., Pedersen, L.H., 2009. Market liquidity and funding liquidity. Review of Financial Studies 22, 2201–2238.

Caballero, R.J., Krishnamurthy, A., 2008. Collective risk management in a flight to quality episode. The Journal of Finance 63, 2195–2230.

Calvo, G.A., Mendoza, E.G., 2000. Rational contagion and the globalization of securities markets. Journal of International Economics 51, 79–113.

Chan, K.F., Treepongkaruna, S., Brooks, R., Gray, S., 2011. Asset market linkages: evidence from financial, commodity and real estate assets. Journal of Banking and Finance 35, 1415–1426.

Chordia, T., Sarkar, A., Subrahmanyam, A., 2005. An empirical analysis of stock and bond market liquidity. Review of Financial Studies 18, 85–130.

Connolly, R., Stivers, C., Sun, L., 2005. Stock market uncertainty and the stockbond return relation. Journal of Financial and Quantitative Analysis 40, 161–194.

Corradi, V., Silvapulle, M.J., Swanson, N.R., 2014. Consistent pretesting for jumps. Working Paper.

De Jong, F., De Roon, F.A., 2005. Time-varying market integration and expected returns in emerging markets. Journal of Financial Economics 78, 583–613.

Dewachter, H., Erdemlioglu, D., Gnabo, J.Y., Lecourt, C., 2014. Intraday impact of communication on euro-dollar volatility and jumps. Journal of International Money and Finance 43, 131–154.

Diamond, D. W Dybvig, P.H., 1983. Bank runs, deposit insurance, and liquidity. Journal of Political Economy 91, 401–419.

Diebold, F.X., Nerlove, M., 1989. The dynamics of exchange rate volatility: a multivariate latent-factor ARCH model. Journal of Applied Econometrics 4, 1–22.

Diebold, F.X., Yilmaz, K., 2014. On the network topology of variance decompositions: Measuring the connectedness of financial firms. Journal of Econometrics 182, 119–134.

Dungey, M., Hvozdyk, L., 2012. Cojumping: Evidence from the US Treasury bond and futures markets. Journal of Banking and Finance 36, 1563–1575.

Dungey, M., Martin, V.L., 2007. Unravelling financial market linkages during crises. Journal of Applied Econometrics 22, 89–119.

Dungey, M., Martin, V.L., Pagan, A.R., 2000. A multivariate latent factor decomposition of international bond yield spreads. Journal of Applied Econometrics 15, 697–715.

Dungey, M., Milunovich, G., Thorp, S., 2010. Unobservable shocks as carriers of contagion. Journal of Banking and Finance 34, 1008–1021.

Ederington, L.H., Lee, J.H., 1993. How markets process information: News releases and volatility. Journal of Finance 48, 1161–1191.

Engle, R., Fleming, M., Ghysels, E., Nguyen, G., 2012. Liquidity, volatility, and flights to safety in the U.S. Treasury market: Evidence from a new class of dynamic order book models. Federal Reserve Bank of New York Staff Reports, no. 590.

Evans, M.D.D., 2002. FX trading and exchange rate dynamics. Journal of Finance 57, 2405–2447.

Favero, C.A., Giavazzi, F., 2002. Is the international propagation of financial shocks non-linear? evidence from the erm. Journal of International Economics 57, 231–246.

Fleming, J., Kirby, C., Ostdiek, B., 1998. Information and volatility linkages in the stock, bond and money markets. Journal of Financial Economics 49, 111–137.

Flood, R.P., Rose, A.K., 2005. Financial integration: A new methodology and an illustration. Journal of the European Economic Association 3, 1349–1359.

Forbes, K., Rigobon, R., 2002. No contagion, only interdependence: measuring stock market co-movements. Journal of Finance 57, 2223–2261.

Forbes, K.J., Chinn, M.D., 2004. A decomposition of global linkages in financial markets over time. The Review of Economics and Statistics 86, 705–722.

Glick, R., Hutchison, M., 2013. China's financial linkages with Asia and the global financial crisis. Journal of International Money and Finance 39, 186–206.

Goyenko, R., Sarkissian, S., 2015. Treasury bond illiquidity and global equity returns. Forthcoming in Journal of Financial and Quantitative Analysis.

Guidolin, M., Timmermann, A., 2006. An econometric model of nonlinear dynamics in the joint distribution of stock and bond returns. Journal of Applied Econometrics 21, 1–22.

Guidolin, M., Timmermann, A., 2007. Asset allocation under multivariate regime switching. Journal of Economic Dynamics and Control 31, 3503–3544.

Hamao, Y. Masulis, R.W., Ng, V.K., 1990. Correlations in price changes and volatility across international stock markets. Review of Financial Studies 3, 281–307.

Hartmann, P., Straetmans, S., de Vries, C.G., 2004. Asset market linkages in crisis periods. The Review of Economics and Statistics 86, 313–326.

Harvey, C.R., Huang, R.D., 1991. Volatility in the foreign currency futures market. Review of Financial Studies 4, 543–569.

Jacod, J., Protter, P., 2011. Discretization of Processes. Springer.

Jacod, J., Todorov, V., 2009. Testing for common arrival of jumps in discretely-observed multidimensional processes. Annals of Statistics 37, 1792–1938.

Jacod, J., Todorov, V., 2010. Do price and volatility jump together? Annals of Applied Probability 20, 1425–1469.

Jiang, G.J., Ingrid, L., Verdelhan, A., 2011. Information shocks, liquidity shocks, jumps, and price discovery: Evidence from the U.S. Treasury market. Journal of Financial and Quantitative Analysis 46, 2010.

Jing, B.Y., Kong, X.B., Liu, Z., Mykland, 2012. On the jump activity index for semimartingales. Journal of Econometrics 166, 213–223.

Kaminsky, G.L., Reinhart, C.M., 2000. On crises, contagion and confusion. Journal of International Economics 51, 145–168.

Kaminsky, G.L., Reinhart, C.M., Végh, C.A., 2003. The unholy trinity of financial contagion. Journal of Economic Perspectives 17, 51–74.

Karolyi, G.A., 1995. A multivariate GARCH model of international transmission of stock returns and volatility: the case of the United States and Canada. Journal of Business and Economic Statistics 13, 11–25.

Karolyi, G.A., Stulz, R.M., 1996. Why do markets move together? An investigation of U.S.-Japan stock return comovements. The Journal of Finance 51, 951–986.

Kim, S.J., Moshirian, F., Wu, E., 2006. Evolution of international stock and bond market integration: influence of the European monetary union. Journal of Banking and Finance 30, 1507–1534.

King, M., Sentana, E., Wadhwani, S., 1994. Volatility and links between national stock markets. Econometrica 62, 901–933.

King, M., Wadhwani, S., 1990. Transmission of volatility between stock markets. Review of Financial Studies 3, 5–33.

Lahaye, J., Laurent, S., Neely, C.J., 2011. Jumps, cojumps and macro announcements. Journal of Applied Econometrics 26, 893–921.

Li, J., Todorov, V., Tauchen, G., 2014. Jump regressions. Discussion Paper, Duke University.

Li, J., Todorov, V., Tauchen, G., Chen, R., 2016. Mixed-scale jump regressions with bootstrap inference. Working Paper.

Lin, W., Engle, R.F., Ito, T., 1994. Do bulls and bears move across borders. Review of Financial Studies 57, 507–538.

Liu, J., Pan, J., 2003. Dynamic derivative strategies. Journal of Financial Economics 69, 401–430.

Longin, F., Solnik, B., 1995. Is the correlation in international equity returns constant. Journal of International Money and Finance 14, 3–26.

Longstaff, F., 2004. The flight-to-liquidity premium in U.S. Treasury bond prices. Journal of Business 77, 511–526.

Maheu, J.M., McCurdy, T.H., Zhao, X., 2013. Do jumps contribute to the dynamics of the equity premium. Journal of Financial Economics 110, 457–477.

Mahieu, R., Schotman, P., 1994. Neglected common factors in exchange rate volatility. Journal of Empirical Finance 1, 279–311.

Mancini, G., Gobbi, F., 2012. Identifying the Brownian covariation from the co-jumps given discrete observations. Econometric Theory 28, 249–273.

Panchenko, W., Wu, E., 2009. Time-varying market integration and stock and bond return concordance in emerging markets. Journal of Banking and Finance 33, 1014–1021.

Pelletier, D., 2006. Regime switching for dynamic correlations. Journal of Econometrics 131, 445–473.

Todorov, V., 2010. Variance risk premium dynamics: The role of jumps. Review of Financial Studies 23, 345–383.

Todorov, V., Tauchen, G., 2010. Activity signature functions for high-frequency data analysis. Journal of Econometrics 154, 125–138.

Todorov, V., Tauchen, G., 2011. Volatility jumps. Journal of Business and Economic Statistics 29, 356–371.

Vayanos, D., 2004. Flight to quality, flight to liquidity, and the pricing of risk. NBER, Working Paper 10327.

Appendices

A. Proofs

The proofs are similar to the (one-dimensional) theorems in Boswijk et al. (2014). This appendix presents the key assumptions and most essential results. We extend the self-excitation (univariate) framework of Boswijk et al. (2014) to the multivariate case. To prove the main theorems, we require the function H to satisfy certain conditions. We start by summarizing these conditions in the following two assumptions.

A.1. Assumptions and main results

Assumption 2. *H is C^1 on $\mathcal{D}(R)\times\mathbb{R}_+^{*2}$ and, for some $q,q'>\max\beta_1,\beta_2$,*

(a) The condition (11) *holds;*

(b) $\frac{1}{|x_2-x_1|^q}H(x_1,x_2,y_1,y_2)$, $\frac{1}{|x_2-x_1|^q}H_3'(x_1,x_2,y_1,y_2)$ and $\frac{1}{|x_2-x_1|^q}H_4'(x_1,x_2,y_1,y_2)$ are locally bounded on $\mathcal{D}(R)\times\mathbb{R}_+^{*2}$;

(c) $\frac{1}{|x|^{q_c'}|x_2-x_1|^{q_d'}}|H(x_1+x,x_2,y_1,y_2)-H(x_1,x_2,y_1,y_2)|$ and $\frac{1}{|x|^{q_c'}|x_2-x_1|^{q_d'}}|H(x_1,x_2+x,y_1,y_2)-H(x_1,x_2,y_1,y_2)|$ are locally bounded for any $x\in\mathbb{R}$.

It is possible that the limiting processes $\mathcal{U}$ and $\mathcal{U}'$ in the above CLT vanish. We can also consider a situation when X and λ have no common jumps. Additionally, the following *degeneracy condition* holds:

$$y_1=y_2\Longrightarrow\|H_3'(x_1,x_2,y_1,y_2)\|+\|H_4'(x_1,x_2,y_1,y_2)\|=0. \tag{A.1}$$

In this case, we need a higher order CLT, which requires stronger (smoothness) assumptions on H.

Assumption 3. *The function H satisfies part (b) and (c) of Assumption 2 and*

(a) One of (9), (10) *and* (11) *holds.*

(b) $H(x_1,x_2,y_1,y_2)$ is C^1 in (x_1,x_2) and C^2 in (y_1,y_2) on $\mathcal{D}(R)\times\mathbb{R}_+^{*2}$;

(c) $\frac{1}{|x_2-x_1|^p}H_{ij}''(x_1,x_2,y_1,y_2)$ is locally bounded on $\mathcal{D}(R)\times\mathbb{R}_+^{*2}$ for $i,j=3,4$.

We can replace the local boundedness assumptions in Assumptions 1 by boundedness. This can be done in a localization procedure, a standard approach in high frequency econometrics (see e.g., Jacod and Protter, 2011). We have the following assumption:

Assumption 4. *The processes b and σ are both bounded by some constant L, and Assumption 1 holds with $L_t(\omega)=L$, hence λ is also bounded by L. Furthermore, $\delta(\omega,t,x)\le\gamma(x)$, where $\gamma(\cdot)$ is a nonnegative bounded function satisfying $\int_{\mathbb{R}}\big(\gamma(x)^\beta\wedge1\big)F_t(dx)<\infty$, uniformly in t.*

We have the following intermediate result from Boswijk et al. (2014):

Proposition 3. *Suppose X (either X_1 or X_2 or both) satisfy assumption 1 and the following condition hold*

$$1-\varpi\beta<\rho<(1-\varpi\beta)+2\phi'\wedge2\phi''\wedge\frac{1}{2}\varpi\beta. \tag{A.2}$$

Given any finite number of time points $\{t_p\}_{p=1}^P$*, the following vector of random variables:*

$$\sqrt{\frac{k_n\Delta_n}{\Delta_n^{\varpi\beta}}}\left(\widehat{\lambda}(k_n)_{t_p}-\lambda_{t_p}\right)_{1\leq p\leq P}, \tag{A.3}$$

converges stably in law to a vector of Gaussian random variables $(W_{t_p})_{p=1}^P$ *independent of* $\mathcal{F}$*, with*

$$\mathbb{E}_{t_p}(W_{t_p}^2)=\lambda_{t_p}\frac{\alpha^\beta C_\beta(2)}{\big(C_\beta(1)\big)^2} \quad \textit{and} \quad \mathbb{E}_{t_{p\wedge q}}(W_{t_p}W_{t_q})=0.$$

Note that when considering $U(H,k_n)_t^{12}$, we only need to estimate the jump intensity process $\lambda_{2,t}$. Therefore, we replace β by β_2 in condition (A.2), which yields condition (18).

We complete this subsection by introducing some useful notation. We start by decomposing $X_t=X_{d,t}$ ($d=1,2$, which we omit for brevity) as $X_t=X_t^c+X_t^d$, where $X_t^c=X_0+\int_0^t b_s ds+\int_0^t\sigma_s dW_s$, and

$$\begin{aligned}X_t^d&=x\,1_{\{|x|\leq 1\}}*(\mu-\nu)_t+x\,1_{\{|x|>1\}}*\mu_t\\&=x\,1_{\{|x|>\delta\}}*\mu_t+x\,1_{\{|x|\leq\delta\}}*(\mu-\nu)_t-x\,1_{\{\delta<|x|\leq 1\}}*\nu_t\\&=:\ X_t^d(\delta)'+X_t^d(\delta)+B(\delta).\end{aligned}$$

Throughout, we adopt the standard notation (see e.g., Jacod and Todorov, 2010, Aït-Sahalia et al., 2014a and Boswijk et al., 2014). For each integer $m\geq 1$, we define $(S(m,q):q\geq 1)$ to be the successive jump times of the Poisson random measure given by

$$\underline{\mu}^X\left([0,t]\times\left\{x:\frac{1}{m}<\gamma(x)\leq\frac{1}{m-1}\right\}\right).$$

This refers to (5) for $\underline{\mu}^X$ and to Assumption 4 for $\gamma(\cdot)$. One may relabel the two-parameter sequence $(S(m,q):m,q\geq 1)$ to become a single sequence $(T_p:p\geq 1)$ that exhausts the jumps of X. Based on this jump classification, we define

$$\begin{aligned}A_m&=\{z:\gamma(z)\leq 1/m\},\quad \gamma_{m,t}=\int_{A_m}\big(\gamma(x)\big)^\beta F_t(dx),\\ \mathcal{T}_m^t&=\{p:\exists\, p\geq 1 \text{ and } m'\in\{1,\cdots,m\} \text{ s.t. } T_p=S(m',q)\leq[t/\Delta_n]\Delta_n\},\\ i(n,p)&=\text{the unique integer such that } T_p\in(t_{i-1}^n,t_i^n],\\ J(n,m,t)&=\{i(n,p):p\in\mathcal{T}_m^t\},\quad J'(n,m,t)=\{1,\cdots,[t/\Delta_n]\}\setminus J(n,m,t),\\ T_-(n,p)&=t_{i(n,p)-1}^n,\quad T_+(n,p)=t_{i(n,p)}^n,\\ \Omega_{n,m,t}&=\bigcap_{p\neq q,p,q\in\mathcal{T}_m}\{T_p<[t/\Delta_n]\Delta_n-3k_n\Delta_n,\ \text{or } T_p>3k_n\Delta_n \text{ and } |T_p-T_q|>6k_n\Delta_n\}.\end{aligned}$$

Observe that, for any m,

$$\lim_{n\to\infty}\mathbb{P}(\Omega_{n,m,t})=1.$$

We further decompose X as follows

$$X_t = X'(m)_t + L(m)_t + J(m)_t,$$

where

$$b(m)_t = \begin{cases} b_t - \int_{(A_m)^c} xF_t(dx) & \text{if } \beta > 1 \\ b_t, & \text{if } \beta \leq 1, \end{cases} \quad L(m)_t = \begin{cases} \int_0^t \int_{A_m} x(\mu - \nu)(ds, dx) & \text{if } \beta > 1 \\ \int_0^t \int_{A_m} x\mu(ds, dx), & \text{if } \beta \leq 1, \end{cases}$$

$$X'(m) = X_0 + \int_0^t b'(m)_s ds + \int_0^t \sigma_s dW_s, \quad J(m)_t = \int_0^t \int_{(A_m)^c} x\mu(ds, dx).$$

In the sequel, let K be a finite positive number, the value of which may vary from line to line.

A.2. Proof of Theorem 1

Following the arguments in Boswijk et al. (2014), we decompose $U(H, k_n)$ (we omit the superscript "12" for simplicity) into two parts, on the set $\Omega_{n,m,t}$ (with $X = X_1$). That is,

$$U(H, k_n) = \widetilde{U}^n(m) + \overline{U}^n(m),$$

with

$$\begin{cases} \widetilde{U}^n(m)_t = \sum_{p \in \mathcal{T}_m^t} H(X_{i(n,p)-1}, X_{i(n,p)}, \widehat{\lambda}(k_n)_{p-}, \widehat{\lambda}(k_n)_{p+})\, 1_{\{|\Delta^n_{i(n,p)} X| > \alpha \Delta_n^{\varpi}\}}, \\ \overline{U}^n(m)_t = \sum_{j \in J'(n,m,t)} H(X_{j-1}, X_j, \widehat{\lambda}(k_n)_{j-k_n-1}, \widehat{\lambda}(k_n)_j)\, 1_{\{|\Delta^n_j X| > \alpha \Delta_n^{\varpi}\}}. \end{cases}$$

Here, we omit the subscripts for simplicity, i.e., $X = X_1$ and $\lambda = \lambda_2$. The *continuous mapping theorem* yields that, for any m and t,

$$\widetilde{U}^n(m)_t \xrightarrow{\mathbb{P}} \widetilde{U}(m)_t := \sum_{p \in \mathcal{T}_m^t} H(X_{T_{p-}}, X_{T_{p+}}, \lambda_{T_{p-}}, \lambda_{T_{p+}})\, 1_{\{\Delta X_{T_p} \neq 0\}}.$$

In addition to $\widetilde{U}(m)$, we also define

$$\overline{U}(m)_t := U_t - \widetilde{U}(m)_t = \sum_{p \notin \mathcal{T}_m^t} H(X_{T_{p-}}, X_{T_{p+}}, \lambda_{T_{p-}}, \lambda_{T_{p+}})\, 1_{\{\Delta X_{T_p} \neq 0\}},$$

where $\overline{U}(m)$ gives the part of the limiting process that is associated with "small" log-price jumps, while $\widetilde{U}(m)$ gives the other part associated with "large" jumps. When the bandwidth is wk_n, we write $\widetilde{U}'^n(m)$ and $\overline{U}'^n(m)$. Note that if condition (a) in the Theorem is satisfied with some $\epsilon > 0$, then one can set $m \geq 2/\epsilon$. Then $\overline{U}^n(m) \equiv 0$ for sufficiently large n and $\overline{U}(m) \equiv 0$.

As in Boswijk et al. (2014) (Steps 1 and 2 in the proof of Theorem 3.2), one can prove that

$$\sqrt{\frac{k_n \Delta_n}{\Delta_n^{\varpi\beta_2}}} \Big(\widetilde{U}^n(m)_t - \widetilde{U}(m)_t, \widetilde{U}'^n(m)_t - \widetilde{U}(m)_t \Big) \xrightarrow{\mathcal{L}_{st.}} \Big(\mathcal{U}_t, \frac{1}{w}(\mathcal{U}_t + \sqrt{w-1}\, \mathcal{U}'_t) \Big),$$

where

$$\begin{cases} \mathcal{U}_t = \sum_{p\in\mathcal{T}^t} \big(H_3'(X_{T_p-}, X_{T_p+}, \lambda_{T_p-}, \lambda_{T_p})W_p^- + H_4'(X_{T_p-}, X_{T_p+}, \lambda_{T_p-}, \lambda_{T_p})W_p^+\big), \\ \mathcal{U}_t' = \sum_{p\in\mathcal{T}^t} \big(H_3'(X_{T_p-}, X_{T_p+}, \lambda_{T_p-}, \lambda_{T_p})W_p^{'-} + H_4'(X_{T_p-}, X_{T_p+}, \lambda_{T_p-}, \lambda_{T_p})W_p^{'+}\big), \end{cases} \tag{A.4}$$

and we refer to Boswijk et al. (2014) for the details. According to the discussion therein, the limiting process $\mathcal{U}_t$ of $U(H,k_n)_t$ is a Gaussian martingale conditional on the filtration generated by $\{X_{1,s}\}_{s\geq t}$ and $\{X_{2,s}\}_{s\geq t}$ with conditional variance given by

$$\widetilde{\mathbb{E}}((\mathcal{U}_t)^2|\mathcal{F}) = \frac{\alpha^\beta C_\beta(2)}{\big(C_\beta(1)\big)^2} \sum_{s\leq t} \big(\lambda_{s-} H_3'(X_{s-}, X_s, \lambda_{s-}, \lambda_s)^2 + \lambda_s H_4'(X_{s-}, X_s, \lambda_{s-}, \lambda_s)^2\big).$$

We can approximate this limiting variance process by $U(G,k_n)_t$, where the function G is given by (20). Also, $U(G,k_n)_t$ is a consistent estimator of the limiting conditional variance. Then, the statistic t^{12} defined in (19) converges stably in law to a standard normal random variable under the null hypothesis **(A)**. While under H_1 of **(A)**, the calculations in Boswijk et al. (2014) show that it will diverge to infinity with probability one. This completes the proof of part (a) of the theorem.

Under the conditions of part (b), the remaining part of the proof is that, for all $t<\infty$ and $\eta>0$, we have

$$\lim_{m\to\infty} \limsup_{n\to\infty} \mathbb{P}\Big(\sqrt{\frac{k_n\Delta_n}{\Delta_n^{\varpi\beta_2}}}\,\big|\overline{U}^n(m)_t - \overline{U}(m)_t\big| > \eta\Big) = 0, \tag{A.5}$$

and the same for $\overline{U}'^n(m)_t - \overline{U}(m)_t$. Nevertheless, it is enough to prove (A.5) only.

Define $Y(m) = X'(m) + L(m)$, i.e., the sum of continuous component and "small" jumps of X. Hence, for any $i\in J'(n,m,t)$, we have $\Delta_i^n Y(m) = \Delta_i^n X$. Consequently, we can rewrite $\overline{U}^n(m)_t$ as

$$\overline{U}^n(m)_t = \sum_{i\in J'(n,m,t)} H(X_{i-1}, X_{i-1}+\Delta_i^n Y(m), \widehat{\lambda}(k_n)_{j-k_n-1}, \widehat{\lambda}(k_n)_j)\, 1_{\{|\Delta_i^n Y(m)|>\alpha\Delta_n^{\varpi}\}}.$$

As in Boswijk et al. (2014), we introduce the following random variables

$$\begin{aligned}
\bar{\chi}(m,2)_i^n &= H(X_{i-1}, X_{i-1}+\Delta_i^n Y(m), \lambda_{i-1}, \lambda_i)\, 1_{\{|\Delta_i^n Y(m)|>\alpha\Delta_n^{\varpi}\}} \\
&\quad - \sum_{s\in I(n,i)} H(X_{s-}, X_{s-}+\Delta Y(m)_s, \lambda_{i-1}, \lambda_i)\, 1_{\{|\Delta Y(m)_s|\neq 0\}}. \\
\bar{\chi}(m,4)_i^n &= H(X_{i-1}, X_{i-1}+\Delta_i^n Y(m), \lambda_{i-1}, \lambda_i)\, 1_{\{|\Delta_i^n Y(m)|>\alpha\Delta_n^{\varpi}\}} \\
&\quad - \sum_{s\in I(n,i)} H(X_{s-}, X_{s-}+\Delta Y(m)_s, \lambda_{i-1}, \lambda_i)\, 1_{\{|\Delta Y(m)_s|>\alpha\Delta_n^{\varpi}\}}. \\
\bar{\chi}(m,5)_i^n &= H(X_{i-1}, X_{i-1}+\Delta_i^n Y(m), \lambda_{i-1}, \lambda_i)\, 1_{\{|\Delta_i^n Y(m)|>\alpha\Delta_n^{\varpi}, |\Delta Y(m)_s|>q_n\}} \\
&\quad - \sum_{s\in I(n,i)} H(X_{s-}, X_{s-}+\Delta Y(m)_s, \lambda_{i-1}, \lambda_i)\, 1_{\{|\Delta Y(m)_s|>\alpha\Delta_n^{\varpi}\}},
\end{aligned}$$

where $q_n = [(\alpha\Delta_n^{\varpi})^{-l}]$ for some $l\in(1, 1/(2\varpi\beta_1))$.

Again, following the procedures of Boswijk et al. (2014) (Steps 3 to 6 in the proof of Theorem

3.2), we can prove that for any m

$$\limsup_{n\to\infty}\sqrt{\frac{k_n\Delta_n}{\Delta_n^{\varpi\beta_2}}}\sum_{i\in J'(n,m,t)}\mathbb{E}\Big(\big|\overline{U}^n(m)-\sum_{i\in J'(n,m,t)}\bar{\chi}(m,4)_i^n\big|\Big)=\limsup_{n\to\infty}K\gamma_m\Delta_n^{(1-\rho)+(1-\varpi\beta_2)}=0.$$

The last equality holds because we choose $\rho<1$,$\varpi<1/2$ and by default $\beta_2\le 2$ in our analysis.

Note that the evaluations of $\bar{\chi}(m,2)_i^n$, $\bar{\chi}(m,4)_i^n$ and $\bar{\chi}(m,5)_i^n$ are slightly different from those in Boswijk et al. (2014). For brevity, we omit most calculations here and only highlight the differences. We can replace the results given in (B.6) and (B.7) in Boswijk et al. (2014) by the following

$$\begin{aligned}\mathbb{E}\big(\big|\bar{\chi}(m,2)_i^n-\bar{\chi}(m,4)_i^n\big|\big)&\le K\sum_{s\in I(n,i)}\mathbb{E}\big(|\Delta Y(m)_s|^q1_{\{|\Delta Y(m)_s|\le\alpha\Delta_n^{\varpi}\}}\big)\\&\le K\int_{I(n,i)}\int_{\gamma(x)\le\alpha\Delta_n^{\varpi}}\mathbb{E}\big((\gamma(x))^qF_t(dx)ds\big)\\&\le K\Delta_n^{\varpi(q-\beta_1)}\int_{I(n,i)}\int_{A_m}\mathbb{E}\big((\gamma(x))^{\beta_1}F_t(dx)ds\big)\\&\le K\gamma_m\Delta_n^{1+\varpi(q-\beta_1)},\end{aligned}\tag{A.6}$$

and

$$\begin{aligned}&\mathbb{E}\big(\bar{\chi}(m,4)_i^n-\bar{\chi}(m,5)_i^n\big)\\&\le K\,\mathbb{E}\Big(\big(|X_{s-}-X_{i-1}|^{q_c'}+|X_s-X_{i-1}|^{q_c'}\big)\cdot|\Delta_i^nY(m)|^{q_d'}\cdot1_{\{|\Delta Y(m)_s|>q_n\}}\Big)\\&\le K\Big(\mathbb{E}\big(|X_{s-}-X_{i-1}|^{q_c'}+|X_s-X_{i-1}|^{q_c'}\big)^2\cdot\mathbb{E}\big(|\Delta_i^nY(m)|^{2q_d'}\big)\Big)^{1/2}\\&\le K\Delta_n\big(\Delta_n^{(q_c'-1+\varpi(2q_d'-\varpi))/2}+\Delta_n^{\varpi(q_c'+q_d'-\beta_1)}\big)\gamma_m,\end{aligned}\tag{A.7}$$

respectively. Then, it is clear that if $\rho<1-\varpi\beta_2+2\varpi(q-\beta_1)$, we have

$$\begin{aligned}&\lim_{m\to\infty}\limsup_{n\to\infty}\sqrt{\frac{k_n\Delta_n}{\Delta_n^{\varpi\beta_2}}}\sum_{i\in J'(n,m,t)}\mathbb{E}\Big(\big|\bar{\chi}(m,2)_i^n-\bar{\chi}(m,4)_i^n\big|\Big)\\&=\lim_{m\to\infty}\limsup_{n\to\infty}K\gamma_m\Delta_n^{\frac{1}{2}(1-\rho-\varpi\beta_2)+\varpi(q-\beta_1)}=0.\end{aligned}$$

Moreover, as long as $1-\rho-\varpi\beta_2+(q_c'-1+\varpi(2q_d'-\beta_1))\wedge 2\varpi(q_c'+q_d'-\beta_1)\ge 0$,

$$\begin{aligned}&\lim_{m\to\infty}\limsup_{n\to\infty}\sqrt{\frac{k_n\Delta_n}{\Delta_n^{\varpi\beta_2}}}\sum_{i\in J'(n,m,t)}\mathbb{E}\Big(\big|\bar{\chi}(m,4)_i^n-\bar{\chi}(m,5)_i^n\big|\Big)\\&=\lim_{m\to\infty}\limsup_{n\to\infty}K\gamma_m\Delta_n^{(1-\rho-\varpi\beta_2)/2}\big(\Delta_n^{(q_c'-1+\varpi(2q_d'-\varpi))/2}+\Delta_n^{\varpi(q_c'+q_d'-\beta_1)}\big)=0.\end{aligned}$$

Finally, (B.8) in Boswijk et al. (2014) becomes

$$\sum_{i\in J'(n,m,t)}\mathbb{E}\Big(\big|\bar{\chi}(m,5)_i^n\big|\Big)\le K\Delta_n^{\varpi(q\wedge(q_c'+q_d')-\beta_1)}\gamma_m.\tag{A.8}$$

Therefore, if $1-\rho-\varpi\beta_2+\varpi(q\wedge(q'_c+q'_d)-\beta_1)\geq 0$, then we have

$$\lim_{m\to\infty}\limsup_{n\to\infty}\sqrt{\frac{k_n\Delta_n}{\Delta_n^{\varpi\beta_2}}}\sum_{i\in J'(n,m,t)}\mathbb{E}\Big(\big|\bar{\chi}(m,5)_i^n\big|\Big)=0,$$

which concludes the proof.

A.3. Proof of Theorem 2

Step 1. As in Boswijk et al. (2014), the leading term of $\widetilde{U}^n(m)_t$ is given by

$$\begin{aligned}\bar{\xi}_p^n=\frac{k_n\Delta_n}{2\Delta_n^{\varpi\beta}}\Big(&H''_{33}(X_{T_p-},X_{T_p},\lambda_{T_p-},\lambda_{T_p})(\widehat{\lambda}(k_n)_{T_p-}-\lambda_{T_p-})^2\\&+H''_{44}(X_{T_p-},X_{T_p},\lambda_{T_p-},\lambda_{T_p})(\widehat{\lambda}(k_n)_{T_p}-\lambda_{T_p})^2\\&+2H''_{34}(X_{T_p-},X_{T_p},\lambda_{T_p-},\lambda_{T_p})(\widehat{\lambda}(k_n)_{T_p-}-\lambda_{T_p-})(\widehat{\lambda}(k_n)_{T_p}-\lambda_{T_p})\Big),\end{aligned}\tag{A.9}$$

and we obtain the following results:

$$\frac{k_n\Delta_n}{2\Delta_n^{\varpi\beta}}\widetilde{U}^n(m)_t-\sum_{p\in\mathcal{T}_m^t}\bar{\xi}_p^n\xrightarrow{\mathbb{P}}0.$$

$$\sum_{p\in\mathcal{T}_m^t}\bar{\xi}_p^n\xrightarrow{\mathcal{L}_{st.}}\overline{\mathcal{U}}(m)_t.$$

$$\widetilde{\mathbb{E}}(|\overline{\mathcal{U}}(m)_t-\overline{\mathcal{U}}_t|\mid\mathcal{F})\leq K\sum_{s\leq t}|\Delta X_s|^q1_{\{|\Delta X_s|\leq m\}}\leq K\gamma_m t.$$

Then, because we consider the same argument as in the previous proof, we prove part (a) of Theorem 2.

Step 2. Now we turn to part (b). Following the calculations in Boswijk et al. (2014), we can verify that

$$\frac{k_n\Delta_n}{\Delta_n^{\varpi\beta_2}}\sum_i\mathbb{E}\big(\big|\bar{\chi}(m,2)_i^n-\bar{\chi}(m,4)_i^n\big|\big)\leq Kt\gamma_m\Delta_n^{1-\rho-\varpi\beta_2+\varpi(q-\beta_1)},$$

$$\frac{k_n\Delta_n}{\Delta_n^{\varpi\beta_2}}\sum_i\mathbb{E}\big(\big|\bar{\chi}(m,4)_i^n-\bar{\chi}(m,5)_i^n\big|\big)\leq Kt\gamma_m\Delta_n^{1-\rho-\varpi\beta_2+(q'_c-1+\varpi(2q'_d-\beta_1))/2\wedge\varpi(q'_c+q'_d-\beta_1)},$$

$$\frac{k_n\Delta_n}{\Delta_n^{\varpi\beta_2}}\sum_i\mathbb{E}\big(\big|\bar{\chi}(m,5)_i^n\big|\big)\leq Kt\gamma_m\Delta_n^{1-\rho-\varpi\beta_2+\varpi(q\wedge(q'_c+q'_d)-\beta_1)},$$

where the sum $\sum_i$ denotes $\sum_{i\in J'(n,m,t)}$. Under condition (b) of Theorem 2, the three terms above are all asymptotically negligible. Then, the conclusion follows Theorem 3.3 and the arguments of Section 4.3 in Boswijk et al. (2014).

B. Data description and adjustment

30-year US T-bond futures are traded on the Chicago Board of Trade (CBOT). The original time zone for the US bond futures is based on the Eastern time (EST), and we start sampling from 9:35 EST until 16:00 EST, the last observation of the trading day t. These trading hours leave us

$N = 78$ five-minute intervals for the all sample trading days of 30-year US T-bond futures and gold futures.

To correctly match intra-day time intervals, we convert the original time zones to the Greenwich time (GMT) for all asset classes. For the bond futures, we take into account the day sessions as well as the trading at both pit and electronic platforms. We further exclude overnight sessions and apply the automatic rolling method to generate raw database. This method automatically determines the best times to roll of a continuous-time futures price series. The method first computes the daily volume of the both current-month and next-month contracts. Next, the current month contracts are rolled to the next-month contracts, when the volume of the new contracts exceeds the the volume of the current ones. We select the contracts as front futures contracts. Those contracts are the contracts that are closest to maturity. The use of the front contracts allows us to process all nearest contracts into a single continuous contract.

The raw database is based on tick data for all asset classes. We create a database for 5-minute intervals by converting tick-by-tick data into intra-day 5-minute frequencies. For the S&P 500 index data, we consider the business hours (i.e., the day session) as its period of trading activity, and hence start sampling from 9:35 EST until the market closes at 16:00 EST of the trading day t. This corresponds to 14:35−21:00 in GMT with $N = 78$ 5-minute intervals, as in the 30-year T-bond futures data. The emerging market index database covers (i) MSCI EM global index, (ii) MSCI EM Asian index and (iii) MSCI EM Latin index. These indices are based on float-adjusted market capitalization weighted indices to measure the equity market performance of emerging markets (see http://www.msci.com/products/indexes/tools/index.html for the definitions).

Table 1: Signs of the function H for $\Delta\lambda_{2t}$

	$\Delta\lambda_{2t} < 0$	$\Delta\lambda_{2t} = 0$	$\Delta\lambda_{2t} > 0$
H in Equation (9)	+	0	+
H in Equation (10)	0	0	+
H in Equation (11)	-	0	+

Table 2: Testing for the mutual excitation from S&P 500 to Gold

α	*FTS level*	*Jump size*	Flight Cat. (1) (excitation)	Flight Cat. (2) (no excitation)	Flight Cat. (3) (rejecting nulls)	Flight Cat. (4) (accepting nulls)
2	weak	0.001	18.52%	22.22%	7.41%	51.85%
			18.52%	7.41%	11.11%	62.96%
	mild	0.005	29.63%	7.41%	3.70%	59.26%
			18.52%	7.41%	11.11%	62.96%
	severe	0.009	41.67%	8.33%	0.00%	50.00%
			33.33%	8.33%	8.33%	50.00%
3	weak	0.001	18.52%	14.81%	3.70%	62.96%
			14.81%	14.81%	0.00%	70.37%
	mild	0.005	22.22%	11.11%	3.70%	62.96%
			14.81%	14.81%	0.00%	70.37%
	severe	0.009	16.67%	8.33%	0.00%	75.00%
			12.50%	12.50%	0.00%	75.00%
4	weak	0.001	11.11%	11.11%	11.11%	66.67%
			14.81%	11.11%	0.00%	74.07%
	mild	0.005	14.81%	11.11%	7.41%	66.67%
			11.11%	11.11%	0.00%	77.78%
	severe	0.009	8.33%	16.67%	8.33%	66.67%
			8.33%	16.67%	0.00%	75.00%
5	weak	0.001	11.11%	18.52%	11.11%	59.26%
			11.11%	14.81%	3.70%	70.37%
	mild	0.005	3.70%	14.81%	11.11%	70.37%
			7.41%	11.11%	3.70%	77.78%
	severe	0.009	4.17%	16.67%	4.17%	75.00%
			8.33%	16.67%	0.00%	75.00%

Notes: The table presents the test results of the mutual excitation in jumps from asset X (S&P 500) to asset Y (Gold). The first and second columns indicate various diffusion threshold levels (i.e. α) and degree of flights based on different jump sizes (weak/mild/severe), respectively. We consider four categories of testing procedures. Cat. (1): rejecting the null of no mutual excitation and accepting the null of mutual excitation, Cat. (2): accepting the null of no mutual excitation and rejecting the null of mutual excitation, Cat. (3): rejecting the null of no mutual excitation and rejecting the null of mutual excitation, and Cat. (4): accepting the null of no mutual excitation and accepting the null of mutual excitation. The table reports the frequencies (in %) of trading quarters (i.e. 12 weeks) falling into each category. We set $H = H(0;1)$ and $H = H(6;1)$ in upper and lower row frequencies, respectively. The sample covers January 1, 2007 to December 31, 2013 and the sampling frequency is 5-minutes. The significance level of the mutual excitation tests is 0.05.

Table 3: FTS and SRS episodes detected by the mutual excitation tests

	FTS (1)	FTS (2)	FTS (1)	FTS (2)	SRS (1)	SRS (2)	SRS (1)	SRS (2)
Years	$\alpha = 5$	$\alpha = 5$	$\alpha = 2$	$\alpha = 2$	$\alpha = 5$	$\alpha = 5$	$\alpha = 2$	$\alpha = 2$
2007/Q1								
2007/Q2	✓		✓					
2007/Q3	✓		✓				✓	✓
2007/Q4				✓				
2008/Q1								
2008/Q2								
2008/Q3	✓	✓	✓	✓				
2008/Q4								
2009/Q1					✓		✓	✓
2009/Q2								
2009/Q3								
2009/Q4	✓	✓	✓	✓				
2010/Q1					✓	✓	✓	✓
2010/Q2								
2010/Q3								✓
2010/Q4							✓	
2011/Q1	✓	✓						
2011/Q2						✓	✓	✓
2011/Q3			✓	✓			✓	✓
2011/Q4								
2012/Q1			✓	✓				
2012/Q2					✓		✓	✓
2012/Q3				✓	✓		✓	✓
2012/Q4								
2013/Q1								
2013/Q2							✓	
2013/Q3		✓						

Notes: The table presents the flight-to-safety (FTS) and seeking-returns-strategy (SRS) episodes identified by the mutual excitation tests. We report the results for two different types of jump thresholds, $\alpha = 5$ and $\alpha = 2$. We set the jump size as 0.001."✓" denotes the episode of the financial flight detected when the test statistics exceed the critical levels (1.96). On the table, (1) and (2) correspond to measures $H = H(0;1)$ and $H = H(6;1)$ used in the estimations, respectively. For all tests, we consider the null hypothesis of no mutual excitation. The sample covers January 1, 2007 to December 31, 2013 and the sampling frequency is 5-minutes. The significance level of the mutual excitation tests is 0.05.

Table 4: Testing for the mutual excitation from S&P 500 to 30-year US Treasury bonds

α	*FTS level*	*Jump size*	Flight Cat. (1) (excitation)	Flight Cat. (2) (no excitation)	Flight Cat. (3) (rejecting nulls)	Flight Cat. (4) (accepting nulls)
2	weak	0.001	22.22%	7.41%	7.41%	62.96%
			22.22%	14.81%	0.00%	62.96%
	mild	0.005	14.81%	7.41%	7.41%	70.37%
			22.22%	14.81%	0.00%	62.96%
	severe	0.009	16.00%	12.00%	4.00%	68.00%
			24.00%	12.00%	0.00%	64.00%
3	weak	0.001	14.81%	3.70%	0.00%	81.48%
			11.11%	14.81%	0.00%	74.07%
	mild	0.005	11.11%	14.81%	0.00%	74.07%
			11.11%	18.52%	0.00%	70.37%
	severe	0.009	4.00%	20.00%	0.00%	76.00%
			8.00%	20.00%	0.00%	72.00%
4	weak	0.001	7.41%	0.00%	0.00%	92.59%
			0.00%	11.11%	0.00%	88.89%
	mild	0.005	7.41%	11.11%	0.00%	81.48%
			0.00%	18.52%	0.00%	81.48%
	severe	0.009	0.00%	18.52%	0.00%	81.48%
			0.00%	28.00%	0.00%	72.00%
5	weak	0.001	0.00%	0.00%	3.70%	96.30%
			0.00%	18.52%	0.00%	81.48%
	mild	0.005	0.00%	22.22%	3.70%	74.07%
			0.00%	25.93%	0.00%	74.07%
	severe	0.009	0.00%	32.00%	0.00%	68.00%
			0.00%	36.00%	0.00%	64.00%

Notes: The table presents the test results of the mutual excitation in jumps from asset X (S&P 500) to asset Y (30-year US Treasury bond futures). The first and second columns indicate various diffusion threshold levels (i.e. α) and degree of flights based on different jump sizes (weak/mild/severe), respectively. We consider four categories of testing procedures. Cat. (1): rejecting the null of no mutual excitation and accepting the null of mutual excitation, Cat. (2): accepting the null of no mutual excitation and rejecting the null of mutual excitation, Cat. (3): rejecting the null of no mutual excitation and rejecting the null of mutual excitation, and Cat. (4): accepting the null of no mutual excitation and accepting the null of mutual excitation. The table reports the frequencies (in %) of trading quarters (i.e. 12 weeks) falling into each category. We set $H = H(0;1)$ and $H = H(6;1)$ in upper and lower row frequencies, respectively. The sample covers January 1, 2007 to December 31, 2013 and the sampling frequency is 5-minutes. The significance level of the mutual excitation tests is 0.05.

Table 5: FTQ and SRS episodes detected by the mutual excitation tests

	FTQ (1)	FTQ (2)	FTQ (1)	FTQ (2)	SRS (1)	SRS (2)	SRS (1)	SRS (2)
Years	$\alpha = 5$	$\alpha = 5$	$\alpha = 2$	$\alpha = 2$	$\alpha = 5$	$\alpha = 5$	$\alpha = 2$	$\alpha = 2$
2007/Q1			✓			✓	✓	✓
2007/Q2								
2007/Q3			✓	✓			✓	✓
2007/Q4								
2008/Q1							✓	✓
2008/Q2								
2008/Q3								✓
2008/Q4								
2009/Q1								✓
2009/Q2								
2009/Q3								
2009/Q4								
2010/Q1							✓	✓
2010/Q2				✓			✓	
2010/Q3			✓					
2010/Q4							✓	✓
2011/Q1			✓					✓
2011/Q2	✓		✓				✓	
2011/Q3			✓	✓			✓	✓
2011/Q4								
2012/Q1								✓
2012/Q2								
2012/Q3							✓	✓
2012/Q4								
2013/Q1								
2013/Q2			✓	✓				
2013/Q3								✓

Notes: The table presents the flight-to-quality (FTQ) and seeking-returns-strategy (SRS) episodes identified by the mutual excitation tests. We report the results for two different types of jump thresholds, $\alpha = 5$ and $\alpha = 2$. We set the jump size as 0.001."✓" denotes the episode of the financial flight detected when the test statistics exceed the critical levels (1.96). On the table, (1) and (2) correspond to measures $H = H(0;1)$ and $H = H(6;1)$ used in the estimations, respectively. For all tests, we consider the null hypothesis of no mutual excitation. The sample covers January 1, 2007 to December 31, 2013 and the sampling frequency is 5-minutes. The significance level of the mutual excitation tests is 0.05.

Table 6: Testing for the mutual excitation from MSCI index to S&P 500

α	*FTS level*	*Jump size*	Flight Cat. (1) (excitation)	Flight Cat. (2) (no excitation)	Flight Cat. (3) (rejecting nulls)	Flight Cat. (4) (accepting nulls)
2	weak	0.001	25.93%	7.41%	29.63%	37.04%
			22.22%	22.22%	11.11%	44.44%
	mild	0.005	20.00%	40.00%	0.00%	40.00%
			20.00%	40.00%	0.00%	40.00%
	severe	0.009	0.00%	50.00%	0.00%	50.00%
			0.00%	50.00%	0.00%	50.00%
3	weak	0.001	33.33%	7.41%	18.52%	40.74%
			29.63%	11.11%	0.00%	59.26%
	mild	0.005	20.00%	40.00%	0.00%	40.00%
			20.00%	40.00%	0.00%	40.00%
	severe	0.009	0.00%	50.00%	0.00%	50.00%
			0.00%	50.00%	0.00%	50.00%
4	weak	0.001	22.22%	14.81%	3.70%	59.26%
			22.22%	14.81%	0.00%	62.96%
	mild	0.005	20.00%	20.00%	0.00%	60.00%
			20.00%	20.00%	0.00%	60.00%
	severe	0.009	0.00%	50.00%	0.00%	50.00%
			0.00%	50.00%	0.00%	50.00%
5	weak	0.001	25.93%	11.11%	0.00%	62.96%
			18.52%	7.41%	0.00%	74.07%
	mild	0.005	20.00%	0.00%	0.00%	80.00%
			20.00%	0.00%	0.00%	80.00%
	severe	0.009	0.00%	0.00%	0.00%	100.00%
			0.00%	0.00%	0.00%	100.00%

Notes: The table presents the test results of the mutual excitation in jumps from asset X (MSCI) to asset Y (S&P 500 index). The first and second columns indicate various diffusion threshold levels (i.e. α) and degree of integration based on different jump sizes (weak/mild/severe), respectively. We consider four categories of testing procedures. Cat. (1): rejecting the null of no mutual excitation and accepting the null of mutual excitation, Cat. (2): accepting the null of no mutual excitation and rejecting the null of mutual excitation, Cat. (3): rejecting the null of no mutual excitation and rejecting the null of mutual excitation, and Cat. (4): accepting the null of no mutual excitation and accepting the null of mutual excitation. The table reports the frequencies (in %) of trading quarters (i.e. 12 weeks) falling into each category. We set $H = H(0;1)$ and $H = H(6;1)$ in upper and lower row frequencies, respectively. The sample covers January 1, 2007 to December 31, 2013 and the sampling frequency is 5-minutes. The significance level of the mutual excitation tests is 0.05.

Table 7: Testing for the mutual excitation from S&P 500 to MSCI index

α	*FTS level*	*Jump size*	Flight Cat. (1) (excitation)	Flight Cat. (2) (no excitation)	Flight Cat. (3) (rejecting nulls)	Flight Cat. (4) (accepting nulls)
2	weak	0.001	3.70%	40.74%	0.00%	55.56%
			0.00%	25.93%	0.00%	74.07%
	mild	0.005	3.70%	37.04%	0.00%	59.26%
			0.00%	25.93%	0.00%	74.07%
	severe	0.009	4.17%	16.67%	0.00%	79.17%
			4.17%	16.67%	0.00%	79.17%
3	weak	0.001	0.00%	29.63%	0.00%	70.37%
			0.00%	11.11%	0.00%	88.89%
	mild	0.005	0.00%	25.93%	0.00%	74.07%
			0.00%	11.11%	0.00%	88.89%
	severe	0.009	0.00%	4.17%	0.00%	95.83%
			0.00%	4.17%	0.00%	95.83%
4	weak	0.001	0.00%	29.63%	0.00%	70.37%
			0.00%	14.81%	0.00%	85.19%
	mild	0.005	0.00%	25.93%	0.00%	74.07%
			0.00%	14.81%	0.00%	85.19%
	severe	0.009	4.17%	16.67%	0.00%	79.17%
			4.17%	16.67%	0.00%	79.17%
5	weak	0.001	0.00%	14.81%	0.00%	77.78%
			3.70%	14.81%	0.00%	74.07%
	mild	0.005	0.00%	14.81%	0.00%	77.78%
			3.70%	14.81%	0.00%	74.07%
	severe	0.009	8.33%	12.50%	4.17%	70.83%
			8.33%	12.50%	4.17%	70.83%

Notes: The table presents the test results of the mutual excitation in jumps from asset Y (S&P 500 index) to asset X (MSCI index). The first and second columns indicate various diffusion threshold levels (i.e. α) and degree of integration based on different jump sizes (weak/mild/severe), respectively. We consider four categories of testing procedures. Cat. (1): rejecting the null of no mutual excitation and accepting the null of mutual excitation, Cat. (2): accepting the null of no mutual excitation and rejecting the null of mutual excitation, Cat. (3): rejecting the null of no mutual excitation and rejecting the null of mutual excitation, and Cat. (4): accepting the null of no mutual excitation and accepting the null of mutual excitation. The table reports the frequencies (in %) of trading quarters (i.e. 12 weeks) falling into each category. We set $H = H(0;1)$ and $H = H(6;1)$ in upper and lower row frequencies, respectively. The sample covers January 1, 2007 to December 31, 2013 and the sampling frequency is 5-minutes. The significance level of the mutual excitation tests is 0.05.

Table 8: Episodes of asset market integration
between emerging markets (MSCI) and U.S. (S&P 500)

	MSCI $\Longrightarrow$				SPI $\Longrightarrow$			
	SPI (1)	SPI (2)	SPI (1)	SPI (2)	MSCI (1)	MSCI (2)	MSCI (1)	MSCI (2)
Years	$\alpha = 5$	$\alpha = 5$	$\alpha = 2$	$\alpha = 2$	$\alpha = 5$	$\alpha = 5$	$\alpha = 2$	$\alpha = 2$
2007/Q1								
2007/Q2								
2007/Q3			✓					
2007/Q4		✓		✓				
2008/Q1								
2008/Q2		✓	✓					
2008/Q3			✓					
2008/Q4			✓					
2009/Q1			✓	✓				
2009/Q2							✓	
2009/Q3								
2009/Q4	✓	✓	✓	✓				
2010/Q1			✓	✓				
2010/Q2								
2010/Q3								
2010/Q4								
2011/Q1								
2011/Q2	✓		✓					
2011/Q3	✓	✓		✓				
2011/Q4								
2012/Q1			✓	✓				
2012/Q2			✓					
2012/Q3			✓	✓				
2012/Q4								
2013/Q1								
2013/Q2	✓	✓	✓	✓				
2013/Q3			✓					

Notes: The table presents the market integration episodes identified by the mutual excitation tests. We report the results for two different types of jump thresholds, $\alpha = 5$ and $\alpha = 2$. We set the jump size as 0.001."X" denotes the episode of a transition from MSCI to S&P 500 (four left-panels) and S&P 500 to MSCI (four right-panels). We identify the episodes when the test statistics exceed the critical levels (1.96). On the table, (1) and (2) correspond to measures $H = H(0;1)$ and $H = H(6;1)$ used in the estimations, respectively. For all tests, we consider the null hypothesis of no mutual excitation. The sample covers January 1, 2007 to December 31, 2013 and the sampling frequency is 5-minutes. The significance level of the mutual excitation tests is 0.05.

Table 9: Testing for the mutual excitation from (Asia and Latin) MSCI indices to S&P 500

α	*FTS level*	*Jump size*	Flight Cat. (1) (excitation)	Flight Cat. (2) (no excitation)	Flight Cat. (3) (rejecting nulls)	Flight Cat. (4) (accepting nulls)
Panel A. MSCI Asia ⇒ S&P 500						
2	weak	0.001	7.41%	22.22%	7.41%	62.96%
			14.81%	14.81%	0.00%	70.37%
	mild	0.005	14.81%	7.41%	0.00%	77.78%
			14.81%	3.70%	0.00%	81.48%
	severe	0.009	10.00%	20.00%	5.00%	65.00%
			10.00%	10.00%	0.00%	80.00%
5	weak	0.001	0.00%	11.11%	7.41%	81.48%
			3.70%	7.41%	0.00%	88.89%
	mild	0.005	3.70%	11.11%	3.70%	81.48%
			3.70%	11.11%	0.00%	85.19%
	severe	0.009	5.00%	30.00%	10.00%	55.00%
			5.00%	30.00%	0.00%	65.00%
Panel B. MSCI Latin ⇒ S&P 500						
2	weak	0.001	38.46%	3.85%	19.23%	38.46%
			30.77%	11.54%	11.54%	46.15%
	mild	0.005	24.00%	4.00%	16.00%	56.00%
			28.00%	8.00%	12.00%	52.00%
	severe	0.009	21.43%	21.43%	7.14%	50.00%
			28.57%	21.43%	0.00%	50.00%
5	weak	0.10%	15.38%	7.69%	3.85%	73.08%
			19.23%	3.85%	3.85%	73.08%
	mild	0.50%	12.00%	12.00%	4.00%	72.00%
			20.00%	8.00%	4.00%	68.00%
	severe	0.90%	7.14%	14.29%	0.00%	78.57%
			14.29%	7.14%	0.00%	78.57%

Notes: The table presents the test results of the mutual excitation in jumps. Panel A: excitation from Asia MSCI index to S&P 500 index, Panel B: excitation from Asia MSCI index to S&P 500 index. The first and second columns indicate various diffusion threshold levels (i.e. α) and degree of integration based on different jump sizes (weak/mild/severe), respectively. We consider four categories of testing procedures. Cat. (1): rejecting the null of no mutual excitation and accepting the null of mutual excitation, Cat. (2): accepting the null of no mutual excitation and rejecting the null of mutual excitation, Cat. (3): rejecting the null of no mutual excitation and rejecting the null of mutual excitation, and Cat. (4): accepting the null of no mutual excitation and accepting the null of mutual excitation. The table reports the frequencies (in %) of trading quarters (i.e. 12 weeks) falling into each category. We set $H = H(0;1)$ and $H = H(6;1)$ in upper and lower row frequencies, respectively. The sample covers January 1, 2007 to December 31, 2013 and the sampling frequency is 5-minutes. The significance level of the mutual excitation tests is 0.05.

Table 10: Testing for the mutual excitation between volatility jumps and price jumps

Cat. (1) (excitation)	Cat. (2) (no excitation)	Cat. (3) (reject nulls)	Cat. (4) (accept nulls)
Panel A. negative price jumps ⇒ volatility jumps			
37.04%	7.41%	22.22%	33.33%
33.33%	7.41%	7.41%	51.85%
Panel B. positive price jumps ⇒ volatility jumps			
3.70%	40.74%	0.00%	55.56%
0.00%	22.22%	0.00%	77.78%
Panel C. volatility jumps ⇒ price jumps			
37.04%	3.70%	22.22%	37.04%
29.63%	7.41%	14.81%	48.15%

Notes: The table presents the test results of the mutual excitation between volatility and price jumps. Panel A: excitation from negative S&P 500 jumps to VIX index, Panel B: excitation from positive S&P 500 jumps to VIX, Panel C: excitation from VIX jumps to S&P 500. We set the diffusion threshold as $\alpha = 2$. The degree of excitation is 0.001. The table reports the frequencies (in %) of trading quarters (i.e. 12 weeks) falling into each category. We set $H = H(0;1)$ and $H = H(6;1)$ in upper and lower row frequencies, respectively. The sample covers January 1, 2007 to December 31, 2013 and the sampling frequency is 5-minutes. The significance level of the mutual excitation tests is 0.05.

Table 11: Parameter sensitivity of the mutual excitation tests

	Tail prob.	*Excitation prob.*	β	λ	ξ	Size	Power
Base parameters	0.0025	0.80	1.25	20	12	good	good
Varying tail probability							
Sensitivity I	**0.010**	0.80	1.25	62	37	slightly oversized	strong
Sensitivity II	**0.050**	0.80	1.25	223	134	oversized	strong
Varying tail excitation probability							
Sensitivity III	0.0025	**0.90**	1.25	20	14	good	good
Sensitivity IV	0.0025	**0.99**	1.25	20	15	good	good
Varying beta							
Sensitivity V	0.0025	0.80	**1.50**	7	3	slightly undersized	good
Sensitivity VI	0.0025	0.80	**1.75**	4	2	slightly undersized	good

Notes: The table presents the size and power of the mutual excitation tests for different parameter values. *Tail prob.* is the probability of observing a tail shock in an individual asset (i.e., X_1). *Excitation prob.* is the probability that mutual excitation leads a tail event (i.e., from X_1 to X_2). β, λ and ξ denote the jump activity index, jump intensity and excitation parameter, respectively. The last two columns report the empirical size and power of the tests.

Figure 1: S&P 500 and VIX on September 29, 2008

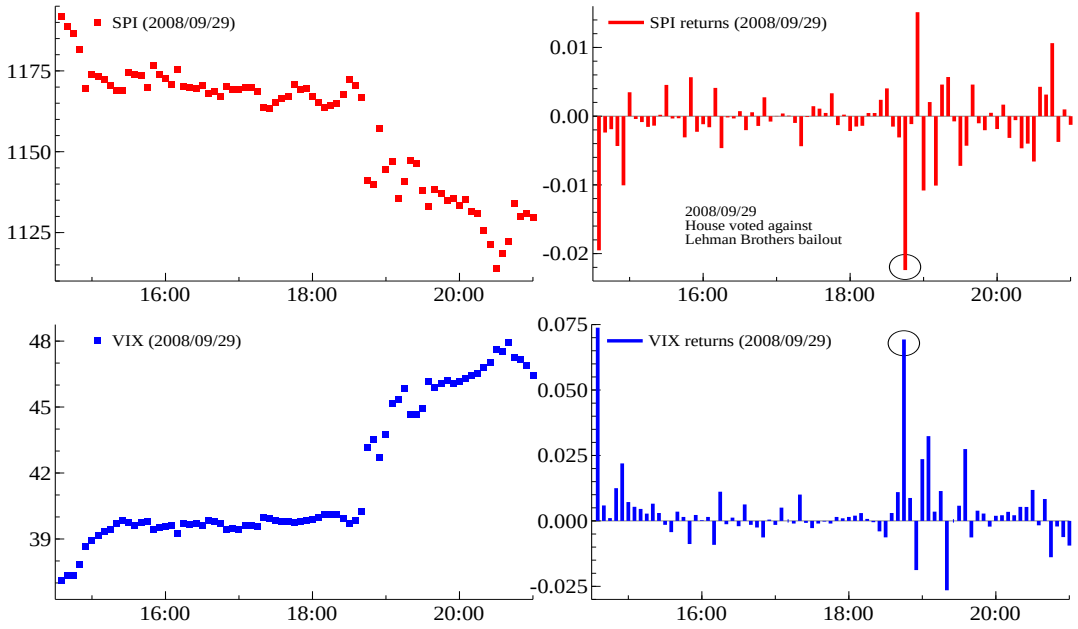

Notes: Illustration of a jump-type event in the VIX index when House voted against the bailout of Lehman Brothers on September 29, 2008: 5-minute intra-day prices (left panels) and log-returns (right panels). The circles on the right panels indicate a detected jump occurring simultaneously around 18:40 GMT.

Figure 2: S&P 500 index and Comex gold spot prices on August 5-6, 2014

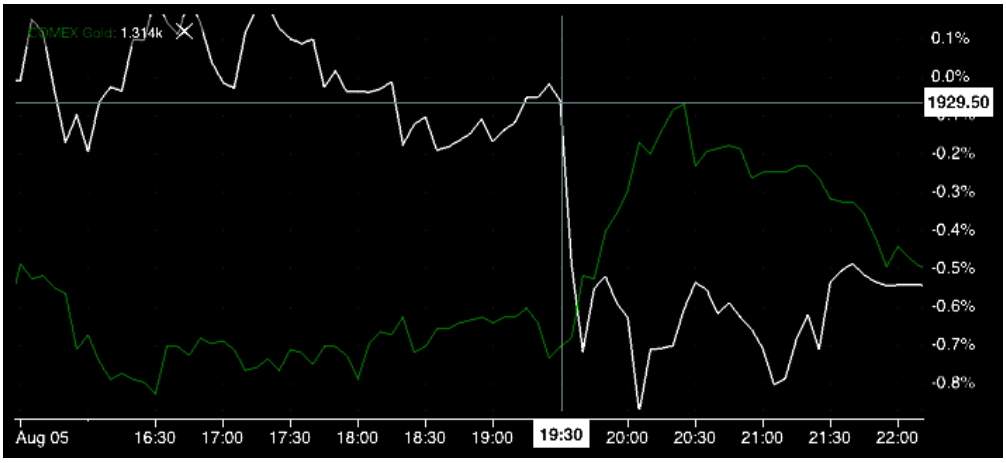

Notes: Illustration of S&P 500 index (white) and Comex gold prices (green) on August 5-6, 2014 when the tension in Middle-east and Ukraine-Russia conflicts increased significantly. Data source and graphics: Bloomberg Analytics.

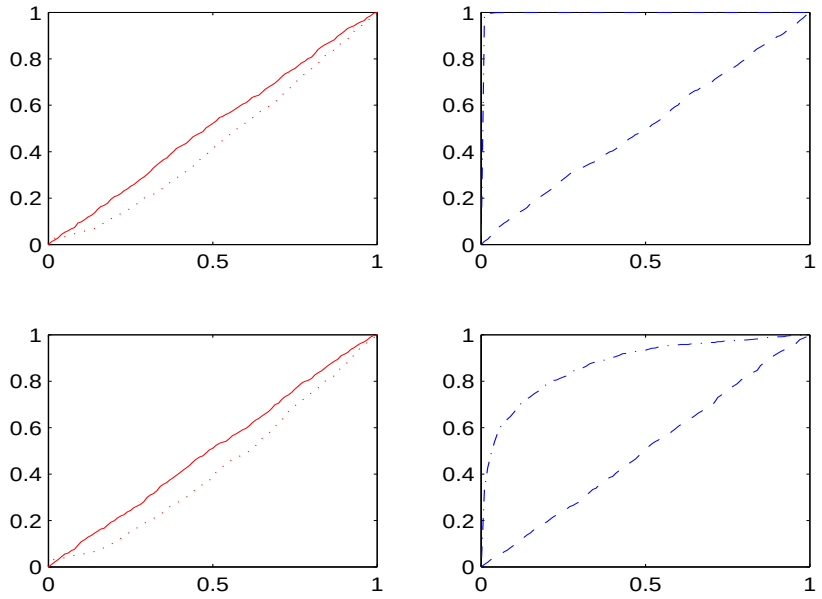

Figure 3: *Notes: Size and power of the tests for mutual-excitation with $\xi = 0$. We set $H = H(0;1)$ in the upper panels and $H = H(6;1)$ in the lower panels. The sampling frequency is 5-seconds. The x-axis shows the nominal level of the test, and the y-axis shows the percentage of rejection in the Monte Carlo sample. Red solid and dotted curves (left panels) correspond to excitation from X_1 to X_2, whereas blue dashed and dotted curves (right panels) correspond to excitation from X_2 to X_1.*

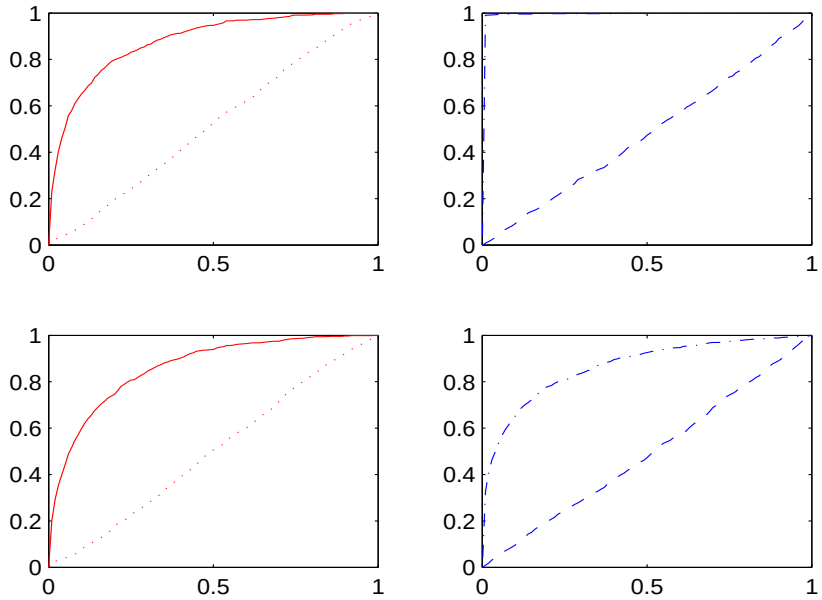

Figure 4: *Notes: Size and power of the tests for mutual-excitation with $\xi = 12$. We set $H = H(0;1)$ in the upper panels and $H = H(6;1)$ in the lower panels. The sampling frequency is 5-seconds. The x-axis shows the nominal level of the test, and the y-axis shows the percentage of rejection in the Monte Carlo sample. Red solid and dotted curves (left panels) correspond to excitation from X_1 to X_2, whereas blue dashed and dotted curves (right panels) correspond to excitation from X_2 to X_1.*

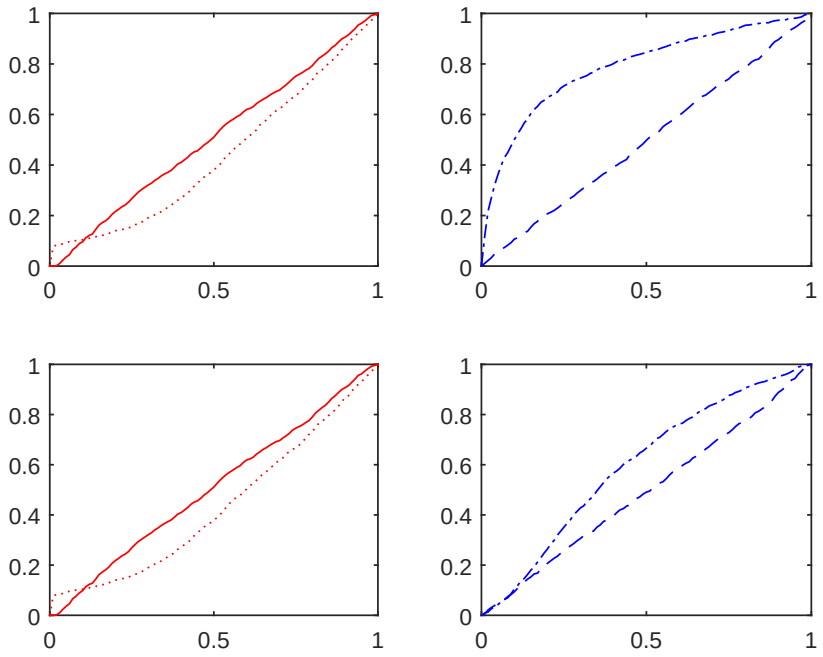

Figure 5: *Notes: Size and power of the tests for mutual-excitation with $\xi = 0$. We set $H = H(0;1)$ in the upper panels and $H = H(6;1)$ in the lower panels. The sampling frequency is 1-minute. The x-axis shows the nominal level of the test, and the y-axis shows the percentage of rejection in the Monte Carlo sample. Red solid and dotted curves (left panels) correspond to excitation from X_1 to X_2, whereas blue dashed and dotted curves (right panels) correspond to excitation from X_2 to X_1.*

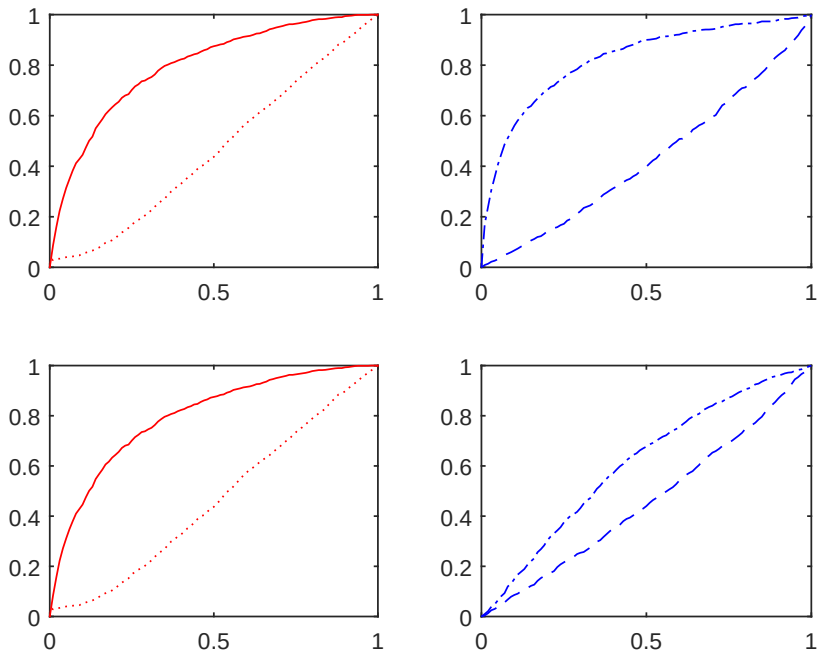

Figure 6: *Notes: Size and power of the tests for mutual-excitation with $\xi = 12$. We set $H = H(0;1)$ in the upper panels and $H = H(6;1)$ in the lower panels. The sampling frequency is 1-minute. The x-axis shows the nominal level of the test, and the y-axis shows the percentage of rejection in the Monte Carlo sample. Red solid and dotted curves (left panels) correspond to excitation from X_1 to X_2, whereas blue dashed and dotted curves (right panels) correspond to excitation from X_2 to X_1.*

Figure 7: Size and power of the tests for financial flights

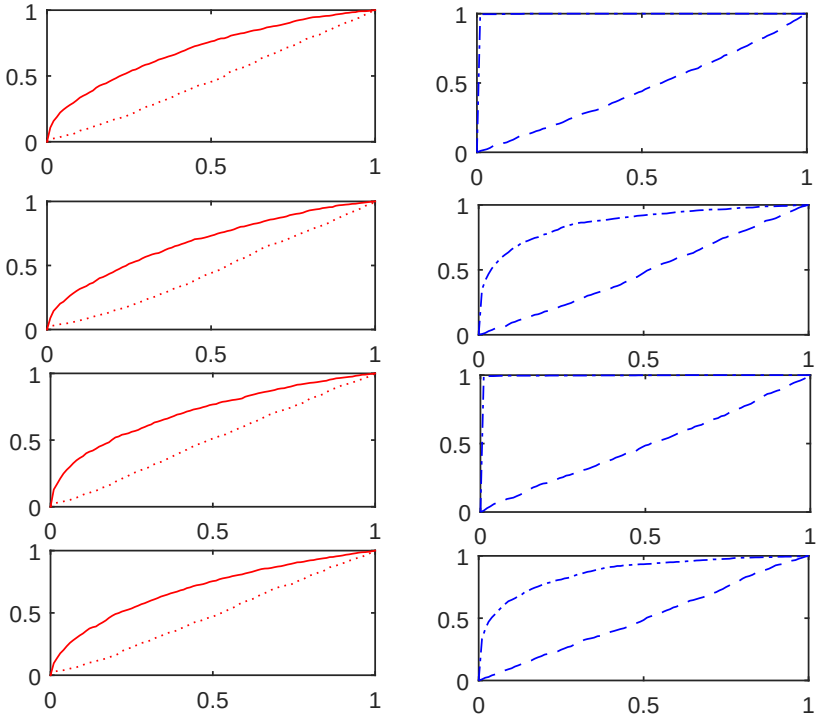

Notes: Size and power of the tests for a financial flight with $\xi = 12$. Two upper-row panels: jump intensity of asset X_2 increases only with negative jumps in asset X_1. Two lower-row panels: jump intensity of asset X_2 increases only with positive jumps in asset X_1. The sampling frequency is 5-seconds. The x-axis shows the nominal level of the test, and the y-axis shows the percentage of rejection in the Monte Carlo sample. Red solid and dotted curves (left panels) correspond to excitation from X_1 to X_2, whereas blue dashed and dotted curves (right panels) correspond to excitation from X_2 to X_1.

Figure 8: S&P 500 (periodicity-filtered) log-returns

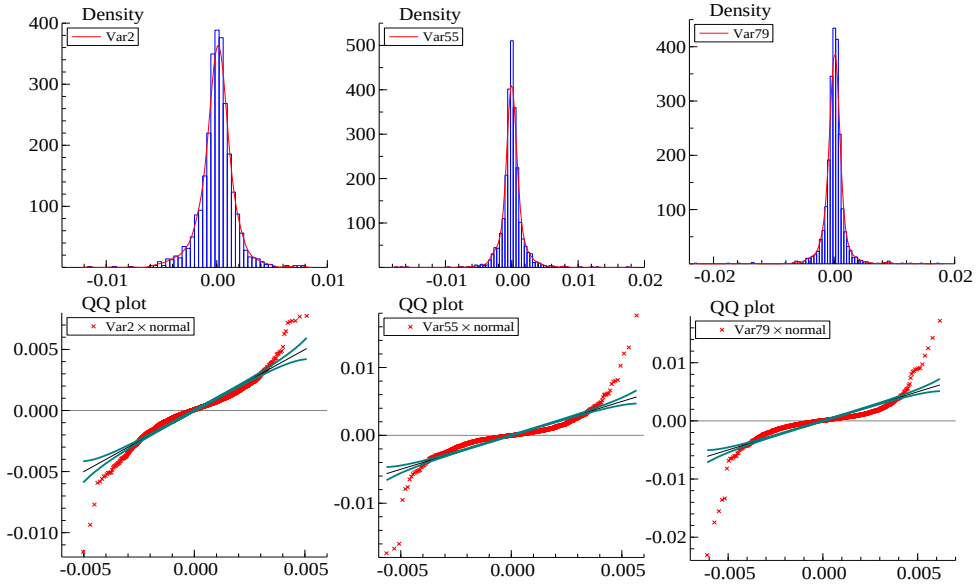

Notes: Empirical densities and QQ plots of S&P 500 (periodicity-filtered) log-returns in different periods of intraday trading: morning (left panels), afternoon (middle panels) and evening (right panels). The sample covers January 1, 2007 to December 31, 2013 and the sampling frequency is 5-minutes.

Figure 9: S&P 500 log-returns

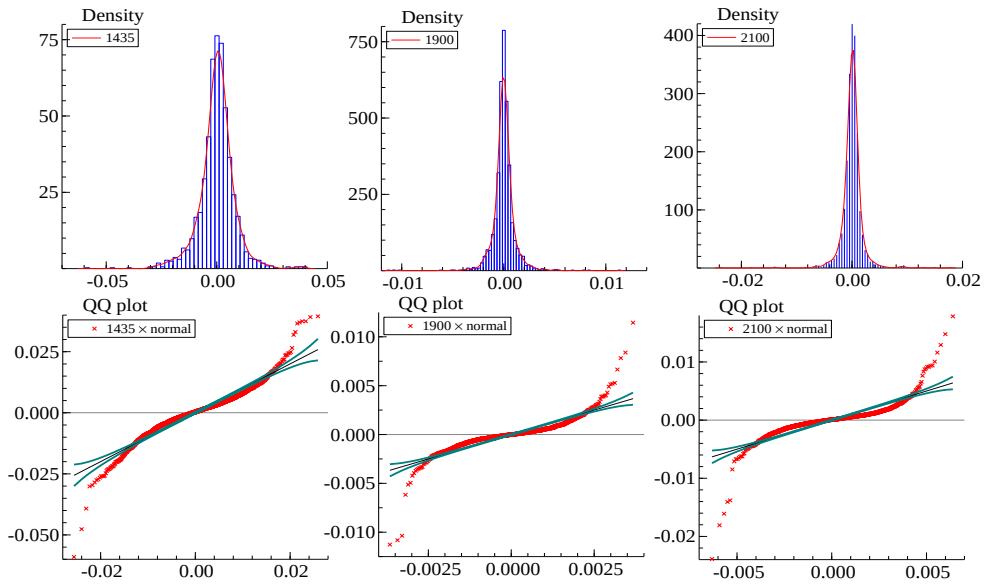

Notes: Empirical densities and QQ plots of S&P 500 log-returns in different periods of intraday trading: morning (left panels), afternoon (middle panels) and evening (right panels). The sample covers January 1, 2007 to December 31, 2013 and the sampling frequency is 5-minutes.

Figure 10: Parameter sensitivity of size and power

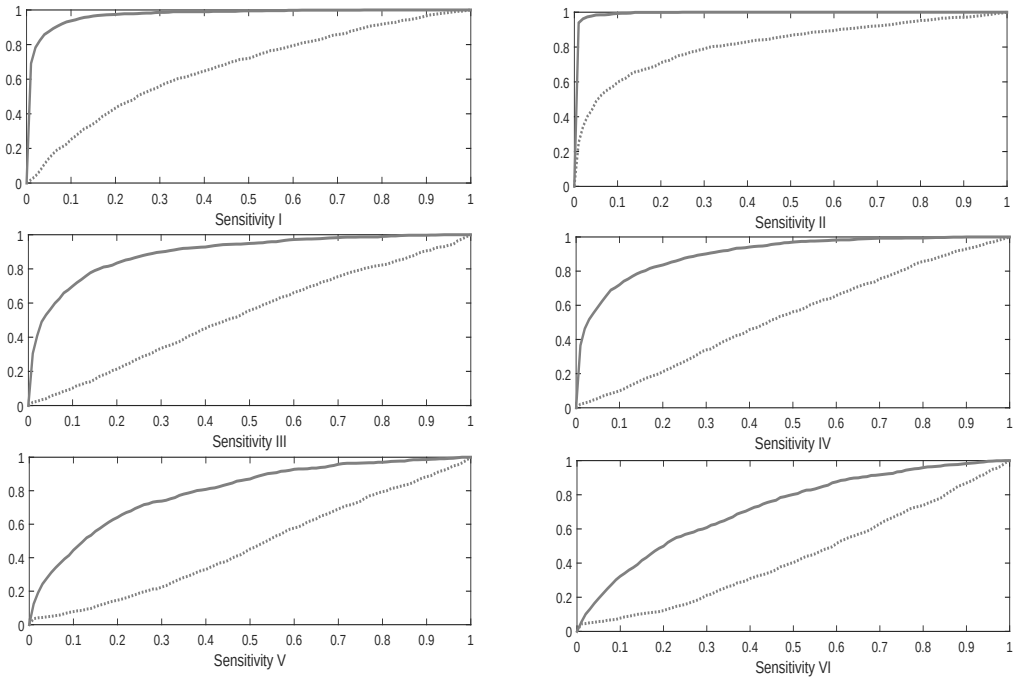

Notes: Size and power of the tests for different parameter values reported in Table 11. We set $H = H(0;1)$ in all panels. The sampling frequency is 5-seconds. The x-axis shows the nominal level of the test, and the y-axis shows the percentage of rejection in the Monte Carlo sample. Gray solid and dotted curves correspond to excitation from X_1 to X_2. See Table 11 for the parameters chosen in each sensitivity analysis, from I to VI.